# CARBON CAPTURE AND STORAGE IN THE ALBERTA OIL SANDS

# A HOLISTIC FRAMEWORK FOR EVALUATING GIGATONNE SCALE GEOLOGICAL $CO_2$ STORAGE IN THE ALBERTA OIL SANDS: PHYSICS, POLICY, AND ECONOMICS

By YU HAO (DAN) ZHAO, B.Eng.Mgt.

A Thesis Submitted to the School of Graduate Studies in Partial Fulfillment of the Requirements for the Degree Master of Applied Science

McMaster University
MASTER OF APPLIED SCIENCE (2023)
Hamilton, Ontario, Canada (Civil Engineering)

| | |
|---|---|
| TITLE: | A holistic framework for evaluating gigatonne scale geological $CO_2$ storage in the Alberta oil sands: physics, policy, and economics |
| AUTHOR: | Yu Hao (Dan) Zhao<br>B.Eng.Mgt. (Civil Engineering and Management),<br>McMaster University, Hamilton, Canada |
| SUPERVISOR: | Dr. Benzhong Zhao |
| NUMBER OF PAGES: | xviii, 65 |

# Lay Abstract

The global community has increasingly recognized the importance of greenhouse gas emission reductions in the effort to mitigate climate change. Carbon capture and storage (CCS) is a technology that, with widespread use at a large scale, has the potential to significantly reduce emissions. However, due to the high cost and lengthy time commitment required, many factors ranging from emission sources to storage capacity to financial considerations must be accounted for to ensure the success of a CCS system. Here, we show that a large-scale CCS system in Alberta is viable and the captured $CO_2$ can be safely stored in the long term. This framework can be used to ensure the success of future CCS projects.

# Abstract

An increasing number of countries worldwide have made commitments in recent years to reduce emissions with the goal of limiting global temperature increases to 1.5-2 °C. Carbon capture and storage (CCS) is capable of significantly reducing anthropogenic carbon dioxide ($CO_2$) emissions and is an important tool in the effort to mitigate climate change. The ability of CCS to sequester emissions at a large scale makes it suitable to particularly emission-intensive sectors, such as the oil and gas sector in Canada. Many factors must be considered holistically to ensure the long-term success of large-scale CCS, such as the availability of emission sources, the design of a $CO_2$ transportation network, the availability and capacity of suitable storage sites, the long-term fate of the injected $CO_2$, the economic viability of the system, and the overall policy environment. Previous studies have considered these factors in demonstrating the viability of CCS in Alberta but have not done so holistically. We take a holistic approach in designing a large-scale integrated CCS system which includes $CO_2$ capture from a hub of 10 large oil sands emitters, transport via a pipeline network, and permanent sequestration in the Nisku and Wabamun saline formations. We use a logistic model to forecast long-term oil sands hydrocarbon production and annual emissions, and ensure that all of the capturable emissions can be stored safely without exceeding pressure limits by modeling the long-term pressure evolution. The

injected $CO_2$ will be fully trapped in 6100-11000 years without migrating past the minimum storage depth. We calculate the capital expenditures for the pipeline and injection well components of the system and show that the amount of funding required is reasonable under the umbrella of federal infrastructure funding. This provides a comprehensive framework to ensure the long-term success of future CCS projects.

*To my loved ones*

# Acknowledgements

I would like to extend my sincerest gratitude to my supervisor, Dr. Benzhong (Robin) Zhao, for his support and assistance throughout this journey. It has been a privilege to work alongside you and none of this would be remotely possible without your guidance. I would also like to extend my sincerest thanks to my committee members and to all of my professors and instructors.

I would also like to thank my friends and colleagues in my lab group, particularly Nima for providing invaluable expertise and Michelle for her unwavering support. This would not have been possible without either of you.

To my family, my partner, and my friends: Thank you for being by my side even when I didn't know I needed your support. Fiona, Kierdra, thank you for reminding me that there is indeed light at the end of the tunnel. To those who I have space to list here (Alanah, Megan, Tate, Regan, Olivia, Katherine), thank you for walking through the rain with me. To everyone else, forgive me for not being able to list you here, but you know who you are.

Lastly, to McMaster University for funding me, for giving me the opportunity to pursue my research, and for being home for eight years: thank you, and I will forever be a Marauder.

# Table of Contents

# List of Figures

# List of Tables

# List of Abbreviations and Symbols

## Abbreviations

| | |
|---|---|
| **ACTL** | Alberta Carbon Trunk Line |
| **CAD** | Canadian dollars |
| **CCS** | Carbon capture and storage |
| **CCUS** | Carbon capture, utilization, and storage |
| **$CO_2$** | Carbon dioxide |
| **EOR** | Enhanced oil recovery |
| **GHG** | Greenhouse gas |
| **GHGRP** | Greenhouse Gas Reporting Program |
| **IPCC** | Intergovernmental Panel on Climate Change |
| **NZA** | Net-Zero Accelerator |
| **NDC** | Nationally determined contribution |

| | |
|---|---|
| **O&M** | Operating and maintenance |
| **PCCC** | Post combustion carbon capture |
| **PCOR** | Plains $CO_2$ Reduction Partnership |
| **TDS** | Total dissolved solids |
| **TIER** | Technology Innovation and Emissions Regulation |
| **USD** | United States dollars |

# Symbols

| | |
|---|---|
| $R$ | Ratio of capturable to total oil sands emissions |
| $Q_{oil}$ | Annual oil production |
| $V_{oil}$ | Total volume of recoverable oil |
| $\alpha$ | Growth rate |
| $t_{peak}$ | Peak time of annual oil production |
| $t$ | Time |
| $I_{CO_2}$ | Emission intensity |
| $E_{total}$ | Projected annual total $CO_2$ emissions |
| $\beta$ | Ratio of CCS hub to total oil sands $CO_2$ emissions |
| $E_{capture}$ | Projected annual capturable $CO_2$ emissions |

| | |
|---|---|
| $H$ | Aquifer thickness |
| $k$ | Permeability |
| $\phi$ | Porosity |
| $S$ | Slope |
| $D$ | Injection well depth |
| $T$ | Aquifer temperature |
| $p_aq$ | Aquifer pressure |
| $p$ | Fluid pressure |
| $c$ | Bulk compressibility |
| $\rho_d$ | Density of supercritical $CO_2$ |
| $\mu_d$ | Viscosity of brine |
| $\mu_{H_2O}$ | Viscosity of water |
| $T^*$ | Equivalent temperature |
| $\chi$ | Mass fraction of $NaCl$ |
| $\mu_g$ | Dynamic viscosity of supercritical $CO_2$ |
| $\rho_w$ | Brine density |
| $\rho_d$ | $CO_2$-saturated brine density |
| $\rho_g$ | Supercritical $CO_2$ density |

| | |
|---|---|
| $\mu_w$ | Brine viscosity |
| $\mu_g$ | Supercritical $CO_2$ viscosity |
| $\sigma$ | Salinity |
| $x$ | Lateral coordinate |
| $Q$ | Volumetric injection rate of $CO_2$ |
| $W$ | Width of the injection well array |
| $l$ | Injection well spacing |
| $q$ | $CO_2$ injection flux |
| $\tilde{h}_g$ | Dimensionless thickness of the $CO_2$ current |
| $\tilde{h}_d$ | Dimensionless thickness of the mound of $CO_2$-saturated brine |
| $\tilde{x}$ | Dimensionless lateral coordinate |
| $\tilde{t}$ | Dimensionless time |
| $T_c$ | Characteristic time |
| $\theta$ | Aquifer slope |
| $S_{wc}$ | Connate water saturation |
| $S_{gr}$ | Residual gas saturation |
| $\lambda_g$ | Mobility of the $CO_2$ current |
| $\lambda_w$ | Mobility of the ambient brine |

| | |
|---|---|
| $\lambda_d$ | Mobility of the dense mound |
| $\mu_g$ | Dynamic viscosity of the $CO_2$ current |
| $\mu_w$ | Dynamic viscosity of the ambient brine |
| $\mu_d$ | Dynamic viscosity of the dense mound |
| $k_{gr}$ | Measured end-point relative permeability of $CO_2$ |
| $\Delta\rho_{dw}$ | Density difference between the dense mound and ambient brine |
| $\Delta\rho_{gw}$ | Density difference between the buoyant $CO_2$ and the ambient brine |
| $q_d$ | Volumetric rate of convective dissolution per unit area of fluid-fluid interface |
| $\chi_v$ | Solubility of $CO_2$ in brine |
| $\rho_d$ | Density of $CO_2$-saturated brine |
| $\rho_g$ | Density of supercritical $CO_2$ |
| $\chi_m$ | Mass fraction of $CO_2$ |
| $M_g$ | Molar mass of $CO_2$ |
| $\rho_w^*$ | Density of pure water |
| $V_\phi$ | Apparent molar volume of $CO_2$ in brine |
| $\forall_{\mathbf{CO_2}}$ | Total volume of injected $CO_2$ |
| $D_{\mathbf{p}}$ | Pipeline inner diameter |

| | |
|---|---|
| $q_{max}$ | Maximum $CO_2$ flow rate |
| $f_f$ | Fanning friction factor |
| $\rho_{\mathbf{CO_2}}$ | Density of $CO_2$ |
| $\Delta P_L$ | Pressure loss along the pipeline segment |
| $L$ | Length of the pipeline segment |
| $Q_{\mathbf{max}}$ | Maximum $CO_2$ flow rate |
| $C$ | Capital cost |

# Declaration of Academic Achievement

The following is a declaration that the work described in this thesis was completed by Yu Hao Zhao with contributions from Dr. Benzhong Zhao and Nima Shakourifar. Yu Hao Zhao contributed to the inception of the study, the design of the work to be done, and was responsible for the review of previous work, data collection, pipeline design, the economic analysis, and the writing of the manuscript. Dr. Benzhong Zhao contributed to the inception of the study, the design of the work to be done, the review of the manuscript, and created the $CO_2$ migration model, and Nima Shakourifar created the pressure model.

# Chapter 1

# Introduction

In recent years, the devastating effects of climate change have become increasingly obvious and have been seen around the world. This has led to an increased focus on climate change mitigation, a field whose focus is on reducing the amount of greenhouse gases (GHGs) emitted into the atmosphere (Anderson & Newell, 2004; Rockström et al., 2009). These gasses are directly responsible for climate change (Falkowski et al., 2000; Hansen & Sato, 2004; Haszeldine, 2009; Kennedy et al., 2009) and the atmospheric GHG level has increased by more than 39% over the past century (Leung et al., 2014) with global surface temperatures increasing around 0.8°C during that time (Leung et al., 2014; National Oceanic and Atmospheric Administration, 2023). Canada is a signatory to the Paris Agreement (United Nations, 2015), a formal global commitment to limit overall global temperature increases to 1.5-2 °C through drastic reductions in GHG emissions. Canada has committed to reducing its annual GHG emissions by 30% of 2005 emission levels by 2030 (Environment and Climate Change Canada, 2021d). More recently, Canada further increased its emissions reduction commitment to a 40-45% reduction compared to 2005 levels in the 2021 Nationally

Determined Contribution (NDC) (Environment and Climate Change Canada, 2021b). Canada emitted 741 megatonnes (Mt) of GHG in 2005 which equates to an emission target of 408-445 Mt in 2030. The most recent modeling shows that Canada is projected to emit 625 Mt of GHG in 2030 (Environment and Climate Change Canada, 2022b) based on emission reduction measures that have already been implemented. Even under the best-case scenario, taking into account emission reduction measures that are planned but not yet implemented, Canada is projected to emit 491 Mt of GHG in 2030 (Environment and Climate Change Canada, 2022b). There is a clear gap between Canada's target and projected emissions and additional action is required to satisfy the NDC commitment.

There are six main sectors, as defined by the Intergovernmental Panel on Climate Change (IPCC), of emission sources in Canada: Energy - Stationary Combustion Sources, Energy - Transport, Agriculture, Energy - Fugitive Sources, Industrial Processes and Product Use, and Waste. These sectors account for 44%, 30%, 8.1%, 7.4%, 7.4%, and 3.8% of 2019 emissions respectively (Environment and Climate Change Canada, 2021c). In particular, the Energy - Stationary Combustion sector emitted 319 Mt of GHG in 2019 (Environment and Climate Change Canada, 2021c) and is by far the largest emitter in the Canadian economy. Much of these emissions come from Oil and Gas Extraction, a subcategory within this sector, which emitted 105 Mt of GHG in 2019. Oil and Gas Extraction is clearly a significant contributor to total Canadian emissions and emitted 14% of total Canadian emissions (Environment and Climate Change Canada, 2021c) in 2019. This is projected to increase to 27% of total Canadian emissions by 2030 (Environment and Climate Change Canada, 2021a).

A technology with significant potential to reduce anthropogenic carbon dioxide

($CO_2$) emissions is carbon capture and storage (CCS). This is a technologically proven technology in which $CO_2$ is captured at stationary point sources and directly injected underground for permanent storage. CCS also includes the subset of carbon capture, utilization, and storage (CCUS) wherein the captured $CO_2$ is utilized in industrial processes such as enhanced oil recovery (EOR) before it is permanently stored. It is commonly accepted that the widespread adoption of CCS will have a significant impact on emission reduction (IPCC, 2018; Leung et al., 2014), with the IPCC (2014) estimating that CCS can account for up to a third of global emissions reductions by 2095 under the best-case scenarios. CCS benefits greatly from emissions from concentrated point sources that can be readily captured (IPCC, 2018; Raza et al., 2019) due to a decrease in cost, thus making it especially suited to industrial processes (Osman et al., 2021). The implementation of large-scale CCS is critical to reducing emission reductions in Canada. This is especially true in the Province of Alberta which houses many industries with significant GHG emissions, in particular the oil and gas sector. We only consider CCS and not CCUS because of the challenges in deploying CCUS as a climate change mitigation technology, such as the absence of a regulatory framework to oversee the transition from oil production to $CO_2$ storage in the case of EOR and the lack of economic benefit from stored $CO_2$ (Bachu, 2016; Ettehadtavakkol et al., 2014)

A large-scale CCS project is an extremely complex undertaking which requires careful consideration of numerous factors that can have a significant impact on its ability to effectively and efficiently reduce emissions. These factors affect all three stages of an integrated CCS system, namely capture, transport, and storage. They include the availability of emissions sources (Hasan et al., 2015; Tapia et al., 2018;

Yu et al., 2019), the design of a $CO_2$ transportation network (Balaji & Rabiei, 2022; Jensen et al., 2013), the availability of suitable storage sites (Budinis et al., 2018; Ciotta et al., 2021; Szulczewski et al., 2012), the safety during injection and long-term fate of the $CO_2$ (Szulczewski et al., 2012), the economic viability of the project (Edwards & Celia, 2018; Leonzio et al., 2019; Tapia et al., 2018; Yao et al., 2018), and a suitable policy environment (Alcalde et al., 2019; Bäckstrand et al., 2011; Romasheva & Ilinova, 2019).

The objective of this thesis is to demonstrate a holistic approach to designing a large-scale integrated CCS system. This type of approach considers future emission projections, emission capture and transport, the pressure- and migration-limited storage capacities of the target geological formation, the total costs of the system, the financing required, and the regulatory and policy environment in which this system will operate. A holistic approach such as this is crucial because of the interdependent nature of each element of this system: the supply of capturable $CO_2$ is forecasted based on future emission projections which then inform the selection of suitable storage formations. These formations must also conform with regulations governing $CO_2$ injection and storage. These elements then dictate the engineering parameters of the $CO_2$ transport pipeline and the characteristics of the injection well array, which must ensure that the storage formation does not fracture and the $CO_2$ migration is limited. The overall cost is a combination of all of these elements, and the regulatory and policy environment must be suitably hospitable.

We follow this holistic approach in designing a large-scale CCS system that captures and transports $CO_2$ from a cluster of emitters in the Athabasca oil sands region of Alberta to deep saline aquifers for permanent storage. In Chapter 2, the literature

pertaining to CCS in Alberta is reviewed and we show that while there have been previous studies done on the subject, they consider only one or a few of the CCS elements described above and do not take a holistic approach. In addition, we discuss the current status of CCS systems in Alberta and show that a gap currently exists due to a lack of large-scale CCS. Chapter 3 identifies the optimal emission source and forecast emissions from this source until the end of the century. Here we also select the target storage formations and determine the relevant formation parameters for use in the modeling. Chapter 4 models the formation pressure increases resulting from large-scale $CO_2$ injection and ensures that the available $CO_2$ can be stored in the target formations without exceeding the regulated pressure limit. Chapter 5 models the post-injection $CO_2$ migration to ensure that the injected $CO_2$ will not migrate beyond the limit established by regulation. In Chapter 6, we design the $CO_2$ transport pipeline to take the most efficient route from the emission source to the storage formations while remaining on land suitable for pipeline construction and operation. The capital costs of the CCS system are calculated in Chapter 7, with the relevant financial and policy incentives discussed as well. Chapter 7 also examines the economic viability of constructing the CCS system from the perspective of the federal government. Areas for further research in subsequent works are discussed in Chapter 8. Finally, Chapter 9 concludes by summarizing key takeaways and identifies areas of further research for subsequent works.

# Chapter 2

# CCS in Alberta

The feasibility of CCS in Alberta has been examined by previous studies. The possibility of capturing $CO_2$ from coal-fired power plants in the Wabamun Lake region and then sequestering it in the Nisku formation has been studied by Eisinger et al. (2011). Jensen et al. (2013) showed that sufficient $CO_2$ sources exist in the Plains $CO_2$ Reduction (PCOR) Partnership region, which includes Alberta, to support a $CO_2$ pipeline. Bachu et al. (2014b) used a volumetric method to estimate the storage capacity of deep Devonian saline aquifers located west of the Athabasca region, Alberta. This method involves multiplying the total pore volume of the aquifers by a simple storage efficiency coefficient (Goodman et al., 2011) to arrive at a high-level storage capacity estimate. Bachu et al. (2014b) showed that sufficient storage capacity is present in this region to support large-scale $CO_2$ sequestration. Another method of estimating storage capacity in saline formations is numerical modeling, which is recommended by Bachu (2007, 2015) for estimations of storage capacities on a local scale. The advantages of this method are that it accounts for the dynamic factors affecting storage capacity as well as site-specific characteristics such as the number and configuration

of injection wells (Bachu, 2007, 2015). While these studies demonstrate the feasibility of CCS in Alberta, they only consider one or a few elements of an integrated CCS system and thus do not take a holistic approach.

The Quest Carbon Capture and Storage Project and the Alberta Carbon Trunk Line (ACTL) system are the two currently operational CCS systems in Alberta. The Quest project captures around 1 Mt of $CO_2$ per year (Duong et al., 2019) from the Shell Scotford Upgrader, a mined oil sands extraction facility (Alberta Department of Energy, 2020). This volume is transported to the Basal Cambrian Sandstone saline aquifer for storage, with a cumulative volume of 27 Mt stored by the end of the project lifespan (Alberta Department of Energy, 2020). The ACTL is a larger-scale CCS system that currently captures 1.6 Mt of $CO_2$ annually and is projected to capture 14.6 Mt of $CO_2$ annually at full capacity (Cole & Itani, 2013). In this system, $CO_2$ capture occurs at industrial emitters located near Edmonton, Alberta, and the captured $CO_2$ is used for EOR before permanent storage (Enhance Energy Inc et al., 2020). The Quest and ACTL projects have demonstrated that CCS in Alberta is feasible, but even at their maximum capacity they are not able to capture and sequester enough $CO_2$ to meet the most recent NDC target. While CCS has significant potential, it is clear that increases in CCS capacity are urgently needed to achieve Canada's emission reduction targets.

The Government of Canada is supportive of increasing domestic CCS capacity. It has committed to developing a comprehensive CCS strategy (Environment and Climate Change Canada, 2020, 2021b, 2022a) and is close to finalizing an investment tax credit that encourages capital investment in large-scale CCS projects (Environment and Climate Change Canada, 2021b, 2022a; Department of Finance Canada). The

federal government has stated that it believes Canada has a comparative advantage in CCS technology and has recently reaffirmed its support for advancing CCS deployment (Environment and Climate Change Canada, 2022a). This support is also reflected at the provincial level, with the government of Alberta announcing its intention to establish carbon sequestration hubs comprised of multiple industrial emission sources (Government of Alberta, 2021). It is clear that the need for and support of large-scale CCS is present at both provincial and federal levels of government.

# Chapter 3

# Emission Sources

Large industrial $CO_2$ emitters in close proximity to each other are attractive for the implementation of large-scale CCS due to greater economies of scale and lower infrastructure costs. The Athabasca oil sands region is home to a number of these emitters.

## 3.1 Emission Clusters

A large emitter is defined by the Government of Alberta as one with annual GHG emissions of greater than 0.1 Mt (Government of Alberta, 2020). We use this as the threshold for inclusion in the analysis and identify all oil sands facilities which reported emissions greater than 0.1 Mt in 2018 to the Canadian Greenhouse Gas Reporting Program (GHGRP) (Government of Canada, 2021b). This list represents the potential emission sources for the CCS system. Three of these facilities are excluded from the analysis because they are located far away from the remaining facilities and it would be economically unviable to include them in the CCS system. From among

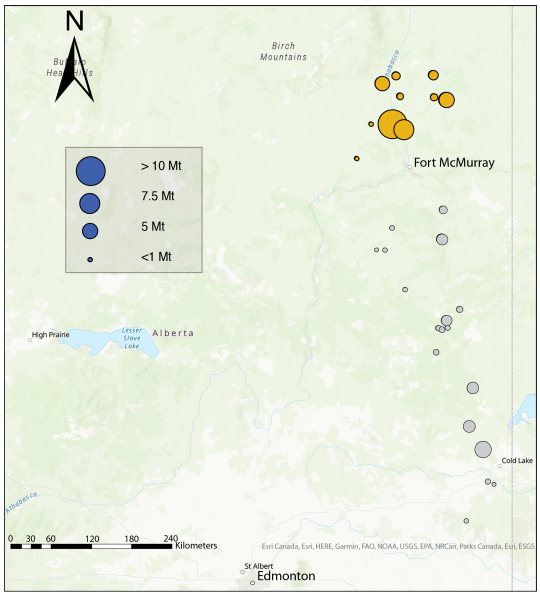


Figure 3.1: Large GHG emitters in the Athabasca oil sands region are shown here with the size of each circle proportional to the facility's GHG emissions in 2018. A hub of 10 facilities (yellow) north of Fort McMurray is particularly attractive for large-scale CCS due to their spatial proximity.

the remaining 29 oil sands facilities (Fig. 3.1), we identify a dense cluster of large emitters north of Fort McMurray. These 10 facilities reported annual emissions of 37.86 Mt in 2018 (Government of Canada, 2021b) (Fig. 3.1), which represents 53% of total oil sands emissions from large emitters. We study the feasibility of building a CCS system around this cluster which is referred to as the CCS hub in the remainder of the work. We focus on the CCS hub because the spatial proximity and large $CO_2$ footprint of these emitters fits the criteria for being attractive for the implementation of large-scale CCS. Ringrose et al. (2021) identifies CCS hubs such as this as a key focus area in the effort to significantly expand $CO_2$ storage.

## 3.2 Carbon Capture Technology

Some of the carbon capture technologies we consider for this system are pre-combustion, post-combustion, and oxy-fuel combustion. We identify post-combustion carbon carbon capture (PCCC) as the optimal choice because it has been used on a global scale and is the most widely used form of carbon capture technology (Chao et al., 2021). In addition, it has been demonstrated at a commercial scale (Bui et al., 2018; Liang et al., 2015), has a lower cost per unit captured compared to other technologies (Mokhtar et al., 2012), and can be readily implemented at existing oil sands facilities (MacDowell et al., 2010; Mokhtar et al., 2012; Zanco et al., 2021). PCCC with the use of amine solvents and solid absorbents is considered to be ready for large-scale commercialization (International Energy Agency, 2020; Kazemifar, 2021; Kearns et al., 2021). This technology is known to have a capture efficiency of 90% (Pilorgé et al., 2020; Porter et al., 2017; Zanco et al., 2021) and can be applied to approximately 88% of $CO_2$ emissions from oil sands operations (Ordorica-Garcia et al., 2011), as emissions from operations such as on-site transportation and maintenance cannot be captured. Thus, the amount of capturable emissions is $R \approx 79\,\%$ of total oil sands emissions.

## 3.3 Emission Projection

Logistic growth models are commonly used to project the depletion of finite resources such as hydrocarbons and groundwater. They have been applied to accurately forecast the growth and decline of oil production (Clark et al., 2011; Hubbert, 1956; Sorrell & Speirs, 2019). We use a logistic growth model to project oil sands hydrocarbon

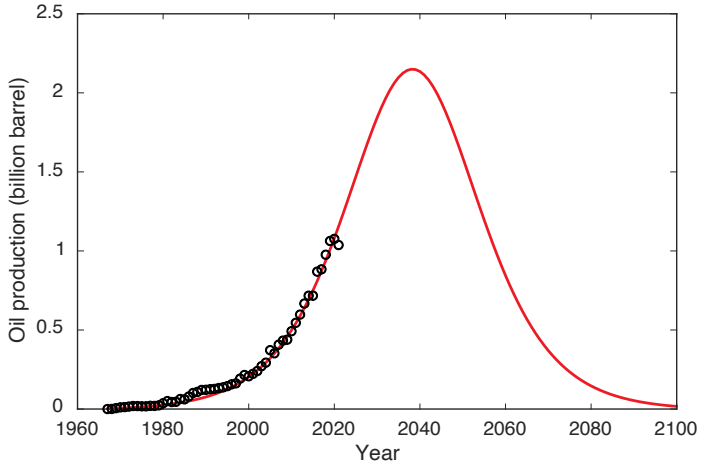


Figure 3.2: A logistic growth model (red line) is used to project future oil sands production in Alberta based on historical production data (black circles). Production is projected to peak in 2038.

production until the end of the century based on historical production data from 1967-2020 (CAPP, 2021), which can then be used to project oil sands emissions until the end of the century. The availability of $CO_2$ is a crucial factor in the design of a CCS system.

The model is of the form:

$$Q_{\text{oil}} = \frac{\alpha \cdot V_{\text{oil}} \cdot \exp(\alpha(t_{\text{peak}} - t))}{(1 + \exp(\alpha(t_{\text{peak}} - t)))^2}, \tag{3.3.1}$$

where $Q_{\text{oil}}$ is the annual oil production (1000s $m^3$/year), $V_{\text{oil}}$ is the total volume of recoverable oil (1000s $m^3$), $\alpha$ is the growth rate (dimensionless), and $t_{\text{peak}}$ is the time at which annual oil production peaks. The logistic growth model perfectly fits the historical annual production data (Fig. 3.2).

To project future $CO_2$ emissions associated with oil sands production, we calculate the amount of $CO_2$ emissions per volume of oil produced based on 2019 emissions data (Government of Canada, 2021b). This gives an average oil sands $CO_2$ emission

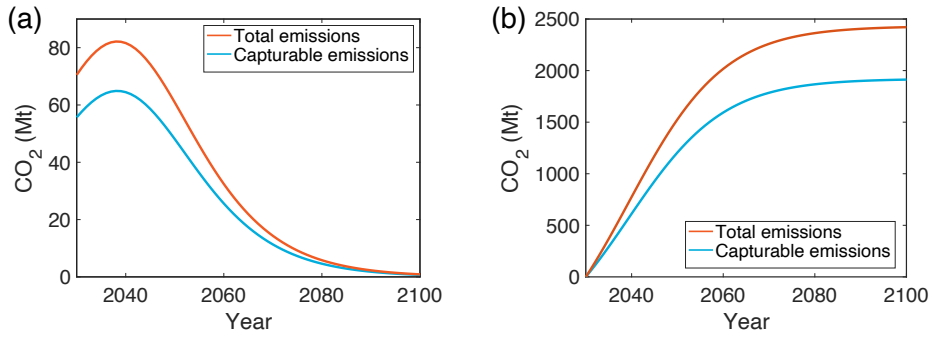


Figure 3.3: (a) Projected annual total and capturable $CO_2$ emissions from the CCS hub. Capturable $CO_2$ emissions peak at 65 Mt in 2038. (b) Projected cumulative total and capturable $CO_2$ emissions from the hub, which will reach 1913 Mt by 2100

intensity $I_{CO_2} = 0.449$ tonnes $CO_2/m^3$ oil produced. The projected annual total $CO_2$ emissions and capturable $CO_2$ emissions due to oil sands production in the proposed CCS hub are therefore given by $E_{\text{total}} = \beta I_{CO_2} Q_{\text{oil}}$ and $E_{\text{capture}} = RE_{\text{total}}$, where $\beta = 53\,\%$ is the ratio of $CO_2$ emissions from the CCS hub to the total oil sands emissions in Alberta, and $R = 79\,\%$ is the percentage of capturable emissions to total emissions. The annual capturable $CO_2$ emission from the CCS hub is projected to peak at 65 Mt in 2038 (Fig. 3.3a). The cumulative capturable $CO_2$ emissions, which represents the total supply of $CO_2$, will reach 1913 Mt by the end of the century if the CCS system begins operation in 2030 (Fig. 3.3b).

## 3.4 Storage Sites and Aquifer Parameters

While the large amount of emissions and resulting $CO_2$ supply from the CCS hub represents significant potential for reducing Canadian emissions, it also poses several challenges for storage options due to the sheer volume of $CO_2$ to be injected and special care must be given to identifying suitable storage formations. We apply the

Table 3.1: Aquifer properties of the Nisku and Wabamun formations (WorleyParsons, 2003; Szulczewski et al., 2012; Bachu et al., 2014a; Ghaderi & Leonenko, 2015; Alberta Geological Survey & Alberta Energy Regulator, 2021).

| Formation | $H$ [m] | $k$ [mD] | $\phi$ [−] | $S$ [−] | $D$ [m] | $T$ [K] | $p_a q$ [mPa] | $c$ [GPa$^{-1}$] |
|---|---|---|---|---|---|---|---|---|
| Nisku | 69 | 49.5 | 0.091 | 0.008 | 1960 | 338 | 19.3 | 0.4 |
| Wabamun | 183 | 42.7 | 0.128 | 0.007 | 1840 | 333 | 18.1 | 0.4 |

following criteria when examining potential storage formations: i) The formation must be more than 1000 m deep, both at the location of injection and throughout the extent of $CO_2$ migration, to align with provincial regulations on $CO_2$ injection; ii) the formation should be thick and have high permeability in order to accommodate the injection of large volumes of $CO_2$; and iii) The formation should be as geographically close to the CCS hub as possible to minimize transport cost. We identify two saline aquifers, namely the Nisku and Wabamun formations, as ideal storage sites. The areal footprints of these formations overlap at the location of injection, which is desirable since only one pipeline would be required to transport the captured $CO_2$.

The Nisku and Wabamun formations are both saline aquifers of the Devonian period. They rise towards the east at an average slope of 7m/km in our study area (Bachu et al., 2014a). The Nisku formation underlies the Calmar formation and overlies the Camrose and Grosmont formations (Bachu et al., 2014a). The Wabamun formation underlies the Banff formation and overlies the Winterburn group (Alberta Geological Survey, 1994a; Bachu et al., 2014a). As mentioned previously, these aquifers both have high permeability and average thickness values which make them ideal for $CO_2$ injection and storage. The other relevant aquifer parameters are summarized in Table 3.1.

Aside from the properties of each aquifer, the properties of the relevant fluids,

namely supercritical $CO_2$ and brine, at aquifer conditions also have an effect on injectivity and storage capacity. Table 3.2 summarizes the fluid properties used in the analysis. We determine the density of supercritical $CO_2$ using a correlation between density, pressure, and temperature based on the method presented by Ouyang (2011) (Eq. 3.4.1) where $b_{i,j}$ are correlation coefficients.

$$\rho_d = A_0 + A_1 p_a q + A_2 p_a q^2 + A_3 p_a q^3 + A_4 p_a q^4 \tag{3.4.1a}$$

$$A_i = b_{i0} + b_{i1} T + b_{i2} T^2 + b_{i3} T^3 + b_{i4} T^4, i = 0, 1, 2, 3, 4 \tag{3.4.1b}$$

We also use Klyukin et al. (2017)'s empirical model (Eq. 3.4.2) to find the viscosity of brine, which is a function of the pressure and temperature at aquifer conditions. This model relates $\mu_d$ at a given pressure, temperature, and $\chi$ to the viscosity of water at the same pressure and an equivalent temperature $T^*$ using fitting coefficients $a_i$ and $b_i$.

$$\mu_d(\chi, T, p) = \mu_{H_2O}(T^*, p) \tag{3.4.2a}$$

$$T^* = e_1 + e_2 T \tag{3.4.2b}$$

$$e_1 = a_1 \chi^{a_2} \tag{3.4.2c}$$

$$e_2 = 1 - b_1 T^{b_2} - b_3 \chi^{a_2} T^{b_2} \tag{3.4.2d}$$

Table 3.2: Fluid properties in the Nisku and Wabamun formations (Bachu et al., 2014a; Ouyang, 2011; Heidaryan et al., 2011).

| Formation | $\rho_w$ [kg/m$^3$] | $\rho_d$ [kg/m$^3$] | $\rho_g$ [kg/m$^3$] | $\mu_w$ [Pa · s] | $\mu_g$ [Pa · s] | $\sigma$ [mg/L] |
|---|---|---|---|---|---|---|
| Nisku | 1180 | 1188 | 675 | $6.33 \times 10^{-4}$ | $5.25 \times 10^{-5}$ | 180000 |
| Wabamun | 1170 | 1178 | 686 | $6.70 \times 10^{-4}$ | $5.32 \times 10^{-5}$ | 170000 |

$\mu_g$ is calculated using an equation from Heidaryan et al. (2011) (Eq. 3.4.3) where $A_i$ are tuned coefficients.

$$\mu_g = \frac{A_1 + A_2 p + A_3 p^2 + A_4 ln(T) + A_5 ln(T)^2 + A_6 ln(T)^3}{1 + A_7 p + A_8 ln(T) + A_9 ln(T)^2} \tag{3.4.3}$$

The density of brine is based on the total dissolved solids (TDS) content of each aquifer and the density of water at aquifer conditions.

# Chapter 4

# Pressure Considerations

The maximum allowable pressure in an aquifer is regulated and is generally a percentage of the aquifer fracture pressure. In Alberta, the aquifer pressure cannot exceed 90% of the formation fracture pressure (AER, 1994). Injecting large amounts of $CO_2$ will cause aquifer pressures to increase, and this pressure increase must be modeled to ensure that it remains under the regulatory limit. Apart from regulatory consequences, exceeding the pressure limit may lead to negative geological impacts on the aquifer itself including the enlargement of existing fractures, the creation of new fractures, or the inducement of seismicity, which may lead to $CO_2$ leakage (Metz et al., 2005). The buildup of pressure in the aquifer is a dynamic quantity that is affected by the rate at which $CO_2$ is injected and can be a limiting factor on $CO_2$ storage. Even if an aquifer has enough capacity to store the cumulative amount of $CO_2$ injected, it may not have sufficient pore spaces to accommodate the required injection rate, which in our study is determined by the projected annual capturable $CO_2$ amount (Fig. 3.3a). An aquifer may thus have a smaller storage capacity that is determined by the maximum injection rate which does not exceed the pressure limit,

which is defined as the pressure-limited storage capacity (Bachu, 2015; Szulczewski et al., 2012).

## 4.1 Pressure Limited Storage Capacity

To determine this pressure-limited storage capacity, the evolution of pressure in the aquifer must be modeled over the injection period. We follow the lead of Bachu (2016) in using the minimum stress pressure rather than the formation fracture pressure as the maximum aquifer pressure, which has the benefit of avoiding the opening of existing fractures in the aquifer in addition to preventing new fractures from forming. Goodarzi et al. (2012) and Bell & Bachu (2003) report a minimum horizontal stress gradient value of 20 kPa/m for the Nisku formation and we assume that this value is also applicable to the Wabamun formation since the Wabamun directly overlies the Nisku at this point and is comprised of the same rock type (Bachu et al., 2014a). We apply the aforementioned regulatory limit of 90% to arrive at pressure limits of 35.3 MPa and 33.1 MPa for Nisku and Wabamun respectively.

We use a line-drive well array with closely-spaced injection wells, which allows pressure evolution to be modeled in the perpendicular dimension to the well array using a simple one-dimensional model while the dimension along the well array is collapsed. The model is a partial differential equation based on conservation of volume and Darcy's law (Eq. 4.1.1) (Pinder & Gray, 2008; Szulczewski et al., 2014). While Szulczewski et al. (2014) have discussed the assumptions of this model, two assumptions in particular should be noted here: i) the compressibility of $CO_2$ at aquifer conditions is equal to that of the ambient brine which results in an overestimation of the pressure increase and a conservative estimate of the pressure-limited

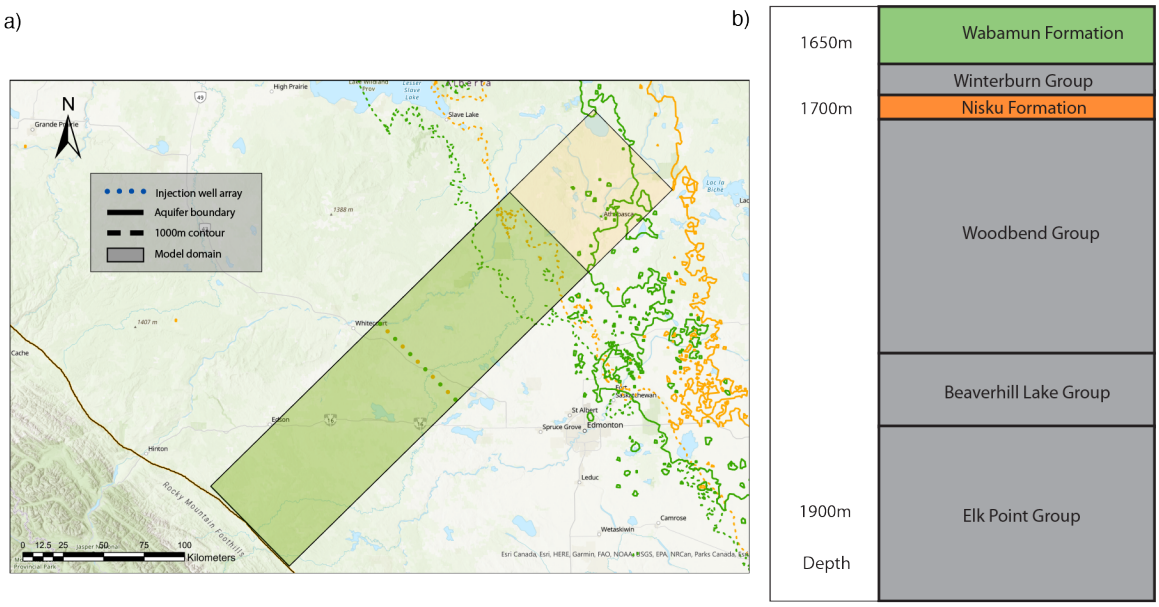


Figure 4.1: (a) The model domains of the Nisku (orange) and Wabamun (green) aquifers. The dotted line represents the injection well array where wells inject alternatively into each aquifer. The solid lines represent the aquifer extents (orange and green) and the data boundary (black), and the dashed lines represent the 1000-m depth contour line. (b) The depths of the Nisku and Wabamun formations in relation to other formations in our study area.

storage capacity, and ii) uniform pressure along the well array (i.e. linear flow) is assumed which is valid if the pressure equilibration between individual wells occurs fairly quickly compared to the overall injection duration (Szulczewski et al., 2012).

The duration of pressure equilibration can be found using Eq. 4.1.2. A well spacing of $l = 2$ km gives $t_{\text{eq}} = 0.7$ years. This value is much smaller than the total injection duration of 71 years, which makes the assumption of uniform pressure along the injection array valid.

$$c\frac{\partial p}{\partial t} - \frac{k}{\mu_w}\frac{\partial^2 p}{\partial x^2} = \frac{Q}{HW}, \tag{4.1.1}$$

$$t_{\text{eq}} = \frac{l^2 c \mu_w}{k}; \tag{4.1.2}$$

## 4.2 Boundary Conditions

The model domain is oriented such that the left and right boundaries are oriented towards the west and the east respectively (Fig. 4.1a). At the left boundary, a stratigraphic cross-section shows that the Nisku formation onlaps onto a dolomite formation, possibly the Duvernay, which then goes on to terminate against the Peace River Arch (Alberta Geological Survey, 1994a). The Wabamun formation experiences a discontinuity as a result of a geologic fault at the left boundary (Alberta Geological Survey, 1994b). We thus assume no-flow boundary conditions for both formations at the left boundary. We assume atmospheric pressure at the right boundaries of both aquifers since they both reach sea level in the domain (Bachu et al., 2014a).

## 4.3 Injection Rates

Equation 4.1.1 is solved numerically under the initial condition assumption of hydrostatic pressure with a finite difference method using fourth-order Runge-Kutta time-stepping.

The $CO_2$ injection flux $q = Q/(HW)$ controls the aquifer pressure increase, which can be thus adjusted by changing $Q$ and $W$. Equation 4.1.1 is solved iteratively to obtain the minimum value of $W$ that meets the aquifer pressure limit while allowing for the entire annual capturable $CO_2$ amount to be stored. A minimum $W$ value is desirable to keep costs as low as possible.

The results suggest that 70% of the annual capturable emissions should be injected into Wabamun and 30% should be injected into Nisku. The entire annual volume can be injected during each year of the injection period while remaining under the pressure limit with $W$=65 km. The aquifer pressures will increase with increasing annual injection volumes until they reach a peak of 32.3 MPa for Wabamun and 31.4 MPa for Nisku in 2053, 24 years after the start of injection (Figure 4.2). A three-dimensional computational model was not used due to the lack of certainty and spatial coverage of the relevant hydrogeologic data in the study area, which mandated the use of the one-dimensional model.

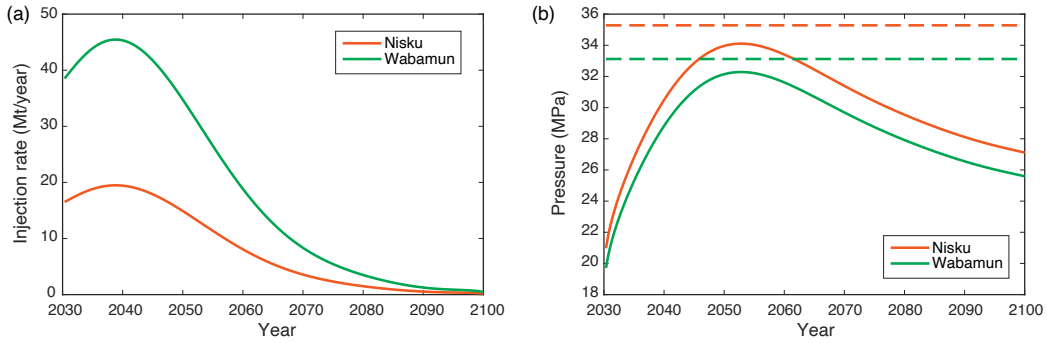


Figure 4.2: (a) Annual $CO_2$ injection rates into the Nisku (orange) and Wabamun (green) formations. The injection rates peak in 2038 due to the peak in emissions at that point and decline thereafter. (b) Aquifer pressure evolution (solid lines) and local maximum pressure limits (dashed lines) in the Nisku (orange) and Wabamun (green) formations. Aquifer pressures are projected to peak in 2053 before declining.

# Chapter 5

# Migration Considerations

The injected $CO_2$ will migrate upward due to buoyancy forces, which occur because $CO_2$ density is less than the density of the ambient brine under aquifer conditions. The $CO_2$ will spread along the caprock as a gravity current, which may be risky due to the possibility of encountering leakage pathways (e.g. faults and abandoned wells). Trapping mechanisms serve to immobilize the $CO_2$ and limit the extent of its migration. These mechanisms include residual trapping, in which portions of $CO_2$ are trapped by capillary forces at the pore scale, and solubility trapping, where $CO_2$ dissolves into the ambient brine and sinks to the aquifer bottom (Hesse et al., 2008; MacMinn et al., 2011). It is necessary to model $CO_2$ trapping to ensure that the migrating $CO_2$ is completely immobilized before it exceeds the regulatory storage depth threshold beyond which $CO_2$ storage is prohibited (Fig. 4.1).

In this study $CO_2$ migration is simulated using a one-dimensional sharp interface model. These models are useful because they can simulate flow over large distances with a lower computational cost than full numerical simulations (Bandilla et al., 2019) and are able to model residual and solubility trapping (Hidalgo et al., 2013).

The model used here is comprised of two coupled partial differential equations that describe the evolution of the buoyant $CO_2$ current and the mound of $CO_2$-saturated brine (the dense mound).

This model is expressed in dimensionless form (Eq. 5.0.1) where $\tilde{h}_g = h_g/H$ and $\tilde{h}_d = h_d/H$ are the local dimensionless thickness of the $CO_2$ current and the thickness of the dense mound, respectively. $\tilde{x} = x/H$ is the dimensionless lateral coordinate and $\theta$ is the aquifer slope. $S_{wc}$ is the connate water saturation, which accounts for the fraction of pore spaces occupied by immobile brine in the wake of $CO_2$. $S_{gr}$ is the residual gas saturation, which represents the fraction of pore spaces occupied by trapped blobs of $CO_2$. Based on relative permeability curves of the Nisku carbonate measured at reservoir conditions it is assumed that $S_{wc} = 0.3$, $S_{gr} = 0.3$ for both formations (Bennion & Bachu, 2008).

$$\frac{\partial \tilde{h}_g}{\partial \tilde{t}} + \frac{1}{(1 - S_{wc} - S_{gr}\tilde{R})} \frac{\partial}{\partial \tilde{x}} \left[ \delta(1 - \tilde{f}_g)\tilde{h}_g(\sin\theta - \cos\theta \frac{\partial \tilde{h}_g}{\partial \tilde{x}}) + \tilde{f}_g \tilde{h}_d(\sin\theta + \cos\theta \frac{\partial \tilde{h}_d}{\partial \tilde{x}})) \right] = -N_d, \tag{5.0.1a}$$

$$\frac{\partial \tilde{h}_d}{\partial \tilde{t}} - \frac{\partial}{\partial \tilde{x}} \left[ \delta \tilde{f}_d \tilde{h}_g(\sin\theta - \cos\theta \frac{\partial \tilde{h}_g}{\partial \tilde{x}}) + (1 - \tilde{f}_d)\tilde{h}_d(\sin\theta + \cos\theta \frac{\partial \tilde{h}_d}{\partial \tilde{x}})) \right] = \frac{N_d}{\chi_v}(1 - S_{wc} - S_{gr}\tilde{R}), \tag{5.0.1b}$$

The discontinuous coefficient $\tilde{R}$ accounts for the fact that residual trapping only occurs where the $CO_2$ gravity current has been displaced by brine. $\tilde{R} = 1$ if $\partial \tilde{h}_g/\partial \tilde{t} < 0$, and $\tilde{R} = 0$ if $\partial \tilde{h}_g/\partial \tilde{t} \geq 0$. $\tilde{f}_g$ and $\tilde{f}_d$ are dimensionless fractional flow functions (Eq. 5.0.2) where $\lambda_g = k k_{gr}/\mu_g$, $\lambda_w = k/\mu_w$, and $\lambda_d = k/\mu_d$ are the mobilities of the $CO_2$ current, ambient brine, and dense mound respectively. $\mu_g$, $\mu_w$, $\mu_d$ are the dynamic

viscosities of the respective fluid phases, and $k_{gr} = 0.55$ is the measured end-point relative permeability of $CO_2$ (Bennion & Bachu, 2008).

$$\tilde{f}_g = \frac{\tilde{h}_g M_g}{\tilde{h}_g(M_{gw} - 1) + \tilde{h}_d(M_{dw} - 1) + 1}, \tag{5.0.2a}$$

$$\tilde{f}_d = \frac{\tilde{h}_d M_d}{\tilde{h}_g(M_{gw} - 1) + \tilde{h}_d(M_{dw} - 1) + 1}, \tag{5.0.2b}$$

$$M_{gw} = \frac{\lambda_g}{\lambda_w}, \tag{5.0.2c}$$

$$M_{dw} = \frac{\lambda_d}{\lambda_w}, \tag{5.0.2d}$$

It is assumed that the dynamic viscosities of the ambient brine and the dense mound are equal and thus $M_{dw} = 1$. Equation 5.0.1 contains dimensionless time $\tilde{t} = t/T_c$, and the characteristic time $T_c$ is given by Equation 5.0.3 where $\Delta\rho_{dw}$ is the density difference between the dense mound and ambient brine.

$$T_c = \frac{H\phi}{\lambda_d \Delta\rho_{dw} g}, \tag{5.0.3}$$

Finally, Equation 5.0.1 contains two additional dimensionless parameters $\delta$ and $N_d$ (Eq. 5.0.4). $\Delta\rho_{gw}$ is the density difference between the buoyant $CO_2$ and the ambient brine. $q_d = \varphi\chi_v\phi\Delta\rho_{dw}g\lambda_d$ is the volumetric rate of convective dissolution per unit area of fluid-fluid interface (Szulczewski et al., 2012), where $\varphi$ is a constant roughly equal to 0.01 (Pau et al., 2010) and $\chi_v = 0.052$ is the solubility of $CO_2$ in brine, expressed as the volume of free-phase $CO_2$ that can be dissolved per unit volume of brine saturated with $CO_2$.

$$\delta = \frac{\lambda_g \Delta\rho_{gw}}{\lambda_d \Delta\rho_{dw}}, \tag{5.0.4a}$$

$$N_d = \frac{q_d}{\lambda_d \Delta\rho_{dw} g\phi}, \tag{5.0.4b}$$

We calculate $\chi_v$ as a function of the density of $CO_2$-saturated brine $\rho_d$, the density of supercritical $CO_2$ $\rho_g$, and the mass fraction of $CO_2$ $\chi_m$ (Szulczewski et al., 2012):

$$\chi_v = \frac{\rho_d}{\rho_g}\chi_m \tag{5.0.5}$$

$\rho_d$ can be calculated as a function of the molar mass of $CO_2$ $M_g$, the density of pure water $\rho_w^*$, and the apparent molar volume of $CO_2$ in brine $V_\phi$, with $V_\phi$ being a correlation dependent on the aquifer temperature in degrees Celsius $T_c$ (Szulczewski et al., 2012):

$$\rho_d = \frac{\rho_w}{1 - \chi_m(1 - V_\phi \rho_w^*/M_g)} \tag{5.0.6a}$$

$$V_\phi = 37.51\text{x}10^{-6} - (9.585\text{x}10^{-8})T_c + (8.740\text{x}10^{-10})T_c^2 - (5.044\text{x}10^{-13})T_c^3 \tag{5.0.6b}$$

The initial condition for the migration model corresponds to the shape of the $CO_2$ plume at the end of the injection period (Nordbotten et al., 2005; Juanes et al., 2010):

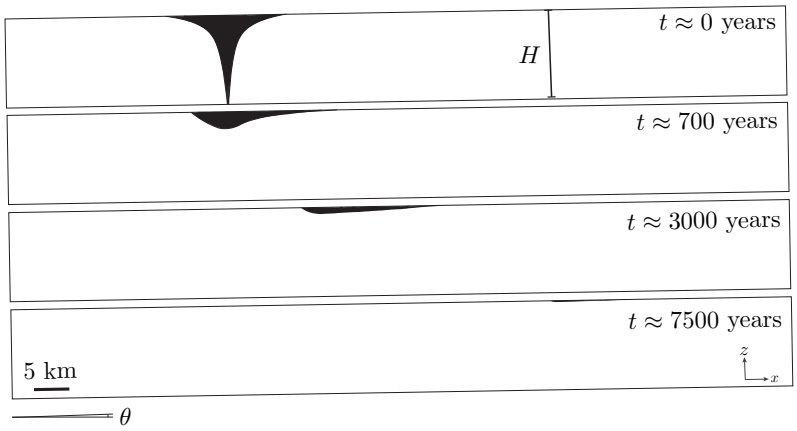


Figure 5.1: Simulation of the $CO_2$ plume profile in the Wabamun formation at the end of the injection period. The volume of mobile $CO_2$ decreases due to residual trapping and solubility trapping. The vertical scale of the aquifer is greatly exaggerated in the figure.

$$\tilde{h}_g = \frac{\sqrt{\frac{M_{gw}}{\tilde{x}/\tilde{l}}} - 1}{M_{gw} - 1}, \tag{5.0.7a}$$

$$\tilde{l} = \frac{V_{CO_2}}{\phi W H^2}, \tag{5.0.7b}$$

where $V_{CO_2}$ is the total volume of injected $CO_2$.

The model indicates that the stored $CO_2$ in the Wabamun formation will be completely immobilized by residual trapping and solubility trapping after about 11000 years. During that time, the $CO_2$ plume will migrate approximately 55 km to the right and 9 km to the left of the well array (Fig. 5.2a). The injected $CO_2$ in the Nisku aquifer will be completely immobilized after about 6100 years and travel approximately 40 km to the right and 9 km to the left of the well array (Fig. 5.2b). In both cases, the regulations surrounding $CO_2$ injection are complied with since the injected $CO_2$ will be fully immobilized before reaching the 1000 m depth contour line of the aquifers.

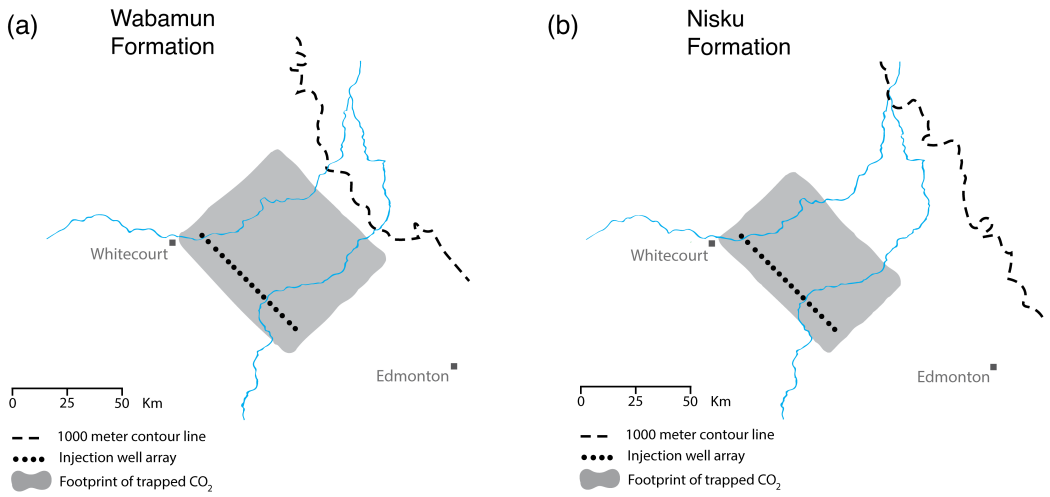


Figure 5.2: (a) shows the $CO_2$ footprint in the Wabamun formation, where it extends ≈9 km to the left and ≈55 km to the right before getting fully trapped. (b) shows the $CO_2$ footprint in Nisku formation. The plume extends ≈40 km to the right and ≈9 km to the left of the well array before getting fully trapped.

# Chapter 6

# Pipeline Design

An extensive pipeline network is required to transport the captured $CO_2$ from the CCS hub to the injection array. We choose to use a trunk-and-branch model to design the pipeline routing, where smaller branch lines connected to each emitter feed into a larger trunk line that connects to the injection array, because it has been shown to provide efficiencies in cost and overall length compared to a traditional point-to-point model (Kuby et al., 2011; Peletiri et al., 2018). The pipeline routing is limited to existing rights-of-way for oil and gas pipelines to ensure that the pipeline only uses land that is suitable for pipeline construction and operation and does not intrude on sensitive areas (e.g. provincial or national parks). We use GIS software to generate potential paths for the pipeline network and manually edit the potential network configurations to arrive at the most efficient one (Edwards & Celia, 2018), defined as the configuration with the shortest overall length (Fig. 6.1).

An important consideration in pipeline design is the diameter, which we determine for each segment in the network based on the expected maximum $CO_2$ flow rate using a modified Darcy-Weisbach equation given by McCollum & Ogden (2006) (Eq. 6.0.1).

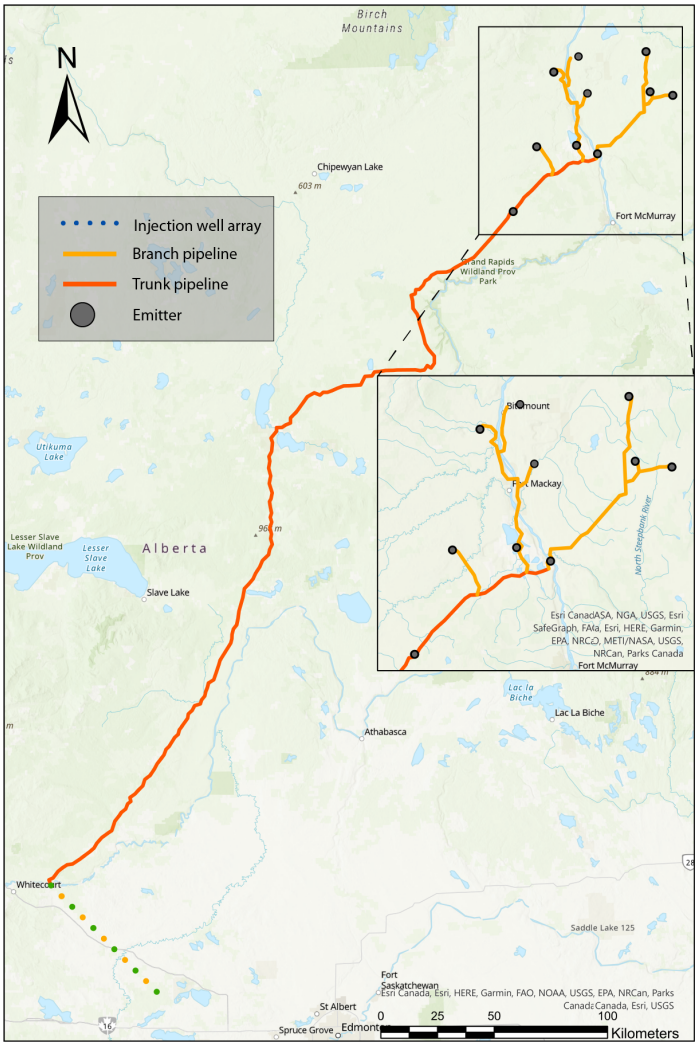


Figure 6.1: The pipeline network follows a trunk-and-branch model and consists of a high-capacity trunk line (orange line) connecting the CCS hub (grey dots) to the injection well array (dotted line) via smaller branch lines (yellow lines).

$$D_{\mathrm{p}} = \left( \frac{32 f_f Q_{\max}^2 L}{\pi^2 \rho_{\mathrm{CO_2}} \Delta P_l} \right)^{0.2}, \tag{6.0.1a}$$

$$\Delta P_l = 6 L Q_{\max}, \tag{6.0.1b}$$

The maximum $CO_2$ flow rate over the operational duration corresponds to the sum of upstream flow during the year of maximum forecasted $CO_2$ emissions. We set the inlet and outlet pressures to 2100 psi and 1400 psi respectively for the trunk line, as these are typical compressor outflow and oilfield delivery pressures (Edwards & Celia, 2018). The branch line outlet pressure is also set to 2100 psi to align with the trunk line inlet pressure. We set the inlet pressure for each branch line to equal the outlet pressure plus $\Delta P_l$, which we calculate using Equation 6.0.1b where $Q_{\max}$ is the maximum $CO_2$ flow in the branch line.

# Chapter 7

# Economic Considerations

This CCS system will be a large-scale infrastructure project. We focus on the capital expenditure of the pipeline network because it is likely to be the largest contributor to the overall capital cost (Edwards & Celia, 2018). Since the $CO_2$ capture equipment will be installed at and operated by each individual facility, we assume that each facility will cover the capital and operational costs associated with $CO_2$ capture.

All costs in this section are in 2025 Canadian dollars (CAD) unless otherwise noted, since construction is assumed to commence in 2025. Costs originally presented in U.S. dollars (USD) are adjusted for inflation using data from the U.S. Bureau of Labor Statistics (2022) and converted to present-day CAD using the average conversion rate over the past five years (Bank of Canada, 2022). The Bank of Canada targets a 1-3% inflation rate (Bank of Canada, 2016) annually. Given the high inflation rates in the current economy, we use 3% to escalate present-day costs to the equivalent in 2025.

## 7.1 Pipeline Cost

We use the NETL $CO_2$ Transport Cost Model (USDOE, 2018) to model the capital cost of pipeline construction. This value is calculated as

$$C = \alpha_{i-0} + L(\alpha_{i-1} D_{\mathrm{p}}^2 + \alpha_{i-2} D_{\mathrm{p}} + \alpha_{i-3}), \tag{7.1.1}$$

where $\alpha_{i-1}, \alpha_{i-2}, \alpha_{i-3}$ are empirical cost parameters determined by fitting the equation to existing pipeline capital cost data (Parker, 2004; USDOE, 2018). Various engineering inputs (Table A.1) affect the empirical cost parameters. The design capacity of each segment is equivalent to the peak upstream $CO_2$ flow.

The pipeline network, consisting of the branch lines, the trunk line, and a pipeline connecting the various injection wells, has a total capital cost of C$4.1 billion (Table 7.1). This number covers the costs of materials, labour, rights-of-way, damages, $CO_2$ surge tanks, a pipeline control system, and pumps but does not include operating and maintenance (O&M).

## 7.2 Injection Well Cost

Another important cost consideration is the cost to drill the various injection wells required as part of the array. The Nisku and Wabamun formations overlap at the location of the injection array (Fig. 4.1b) which enables the use of an overlapping well array. In this design injection wells are spaced 1km apart and alternatively inject into each formation, which provides a significant saving in capital cost since only one pipeline is required for injection into both formations.

$CO_2$ will be injected into the Nisku and Wabamun formations along a 65 km

Table 7.1: Key parameters and capital costs of each pipeline segment and the injection array. Costs have been rounded to two significant figures.

| Pipeline Type | Capital Cost (2025 C$) | Capacity (Mt) | Diameter (in) | Length (km) |
|---|---|---|---|---|
| Branch lines | $42M | 4.68 | 16 | 24 |
| | $8.2M | 2.88 | 16 | 2 |
| | $19M | 9.07 | 16 | 9 |
| | $12M | 11.95 | 16 | 5 |
| | $74M | 16.62 | 20 | 34 |
| | $12M | 29.53 | 24 | 3 |
| | $20M | 3.65 | 12 | 14 |
| | $22M | 8.31 | 16 | 11 |
| | $25M | 11.96 | 16 | 13 |
| | $14M | 2.53 | 12 | 8 |
| | $32M | 14.49 | 16 | 17 |
| | $7.4M | 19.32 | 20 | 2 |
| | $21M | 33.81 | 20 | 8 |
| | $18M | 0.67 | 8 | 15 |
| Trunk line | $3.4B | 64.90 | 48 | 467 |
| Injection array pipeline | $0.4B | 64.90 | 42 | 66 |
| Pipeline cost | $4.1B | | | |
| Injection wells | $0.1B | | | |
| Total capital cost | $4.2B | | | |

long linear well array (Fig. 6.1). Since the Wabamun formation overlaps the Nisku formation (Fig. 4.1b), we design an overlapping injection well array such that only one pipeline is required to connect each injection well. In this design the injection wells are spaced 1 km apart and alternately inject into the Nisku and Wabamun formations. This design represents a significant saving in capital cost over the use of two non-overlapping well arrays as the capital cost of a pipeline is the largest driver of the total cost.

The linear injection array is 65 km long and contains 67 individual injection wells. The capital cost for an injection well in the Nisku formation has been estimated to be C$1.2 million in 2009 (Nygaard & Lavoie, 2009) which is equal to C$1.7 million in 2025. We assume the same cost for an injection well into the Wabamun formation, which is a conservative assumption since the Wabamun overlies the Nisku at this point. The total capital cost of the injection wells is C$0.1 billion. The total capital cost of the system is thus C$4.2 billion, which would be C$3.9 billion in 2022 dollars.

## 7.3 Cost Comparison

To compare pipelines of different lengths and diameters, the cost per inch of diameter per km of length is a commonly used metric. Smith et al. (2021) identify the range of capital costs for onshore $CO_2$ pipelines in 2019US$/in/mile from three sources, which we convert to C$/in/km and escalate to 2025 costs (Table 7.2). Our pipeline network costs C$148,000/in/km, which is within the cost range from the National Petroleum Council (NPC, 2019). To provide additional context, the ACTL has an estimated capital cost of $409,000/in/km (Cole & Itani, 2013).

Table 7.2: Adapted from Smith et al. (2021)

| Capital cost range (2025 C$/in/km) | | | |
|---|---|---|---|
| Low | Mean | High | Source |
| $17,988 | $52,289 | $86,590 | Heddle et al. (2003) |
| $39,596 | $50,993 | $82,925 | USDOE (2018) |
| $79,089 | $113,690 | $148,291 | NPC (2019) |

## 7.4 Financial and Policy Incentives

As we mention previously, both financial and policy incentives are necessary to encourage the widespread adoption of large-scale CCS. It is commonly recognized that a lack of reliable funding to offset the high capital cost is one of the biggest obstacles to large-scale CCS (Alcalde et al., 2019; Boot-Handford et al., 2014; Budinis et al., 2018; Ciotta et al., 2021). The CCS system we propose takes advantage of several financial incentives recently introduced by the Government of Canada that will help offset its capital and operational costs. The Net Zero Accelerator (NZA) initiative aims to support projects that reduce Canadian GHG emissions (Government of Canada, 2021c) and will provide up to C$8 billion towards this end. This initiative is in perfect alignment with the goal of the proposed CCS system because the decarbonisation of large emitters is a key targeted area for support. In addition, the Government of Canada is finalizing an investment tax credit for CCS projects (the CCS Tax Credit) that sequester more than 15 Mt of $CO_2$ annually, which the proposed system does. The draft legislative proposal provides a tax credit of 50% of eligible expenditures related to acquiring $CO_2$ capture equipment between 2022-2030 and 25% between 2031-2040 (Department of Finance Canada). Tax credits for eligible expenditures related to acquiring $CO_2$ transportation and storage equipment are also available at 37.5% between 2022-2030 and 18.75% between 2031-2040 (Department

of Finance Canada), which will directly benefit the facilities capturing $CO_2$ as part of the proposed system.

It is also widely recognized that a supportive policy environment is equally important for the adoption of large-scale CCS (Alcalde et al., 2019; Bäckstrand et al., 2011; Budinis et al., 2018; Romasheva & Ilinova, 2019; Yao et al., 2018). The recently established Clean Fuel Regulation requires a reduction in the carbon intensity of liquid fuels produced and sold in Canada (Department of the Environment, 2020; Government of Canada, 2022). While this regulation directly applies to primary suppliers of liquid fuel (i.e. operators of facilities at which gasoline or diesel is produced) rather than upstream producers of crude oil such as the oil sands extractors included here, these producers are still incentivized to reduce the carbon intensity of their products due to the opportunity to generate credits which can be sold to primary suppliers and other parties to the regulation. The adoption of CCS is noted to be an attractive method to reduce the carbon intensity of fuels (Government of Canada, 2022). At a higher level, the federal government has identified Alberta and Saskatchewan as potential CCS hubs and desires to encourage further CCS deployment by eliminating regulatory barriers and increasing public-private coordination (Government of Canada, 2021a; Environment and Climate Change Canada, 2022a).

There are also incentives available at the provincial level. The Alberta government recently announced that the provincial carbon price will increase to C$170/tonne by 2030 to remain consistent with the federal carbon pricing benchmark (Potkins, 2022). Companies utilizing CCS technology are now also able to generate sequestration credits under the provincial Technology Innovation and Emissions Reduction (TIER) regulation (Potkins, 2022), which offset emissions released into the atmosphere. These

announcements incentivize participation in a CCS hub by both increasing the financial penalty for releasing $CO_2$ emissions into the atmosphere and enabling participants to generate direct value via the sequestration credits.

A potential incentive for the establishment of a CCS system would be the creation of a tax credit similar to the 45Q tax credit established by the United States in 2018. This tax credit provides a set credit amount per tonne of $CO_2$ to emitters who capture and sequester $CO_2$ instead of emitting it into the atmosphere (Congressional Research Service, 2021). While the establishment of a similar tax credit in Canada would not directly impact the capital cost of a CCS system, it would represent an incentive for participation in the system once it is operational. Since it is assumed here that operational costs are borne by each emitter, such a tax credit would provide them with an additional financial credit that directly addresses the operational costs of capturing and storing $CO_2$. A possible source of funding for such a tax credit would be the revenue from the federal carbon price.

## 7.5 Economic Analysis

A private consortium may choose to fund the construction of the proposed pipeline network. They would be able to leverage the federal CCS Tax Credit (Government of Canada, 2021a), which provides a rate of 37.5% for the cost of purchasing and installing eligible equipment incurred between 2022 to 2030. A tariff per tonne of $CO_2$ transported can be implemented once the pipeline becomes operational to offset operational and maintenance expenses.

The federal government may also choose to finance the project completely, which is feasible within the umbrella of federal infrastructure spending. This spending has

risen over the past five years and is projected to continue to rise over the next six years, with the Parliamentary Budget Officer (2022) projecting that the federal government will spend C$32.36 billion on infrastructure in the 2026-2027 fiscal year compared to C$22.778 billion in the 2020-2021 fiscal year. This sum is much greater than the cost of the proposed CCS system, which would be further reduced by being spread over the length of the construction period. The federal government has shown its willingness to invest in large-scale infrastructure projects that address relevant issues such as the GO Transit Expansion Project and the Ontario Line, with investments of nearly C$2 billion in each project (Infrastructure Canada, 2016). Since 2002, the government has made investments of C$1 billion or more in six projects (Infrastructure Canada, 2016) and has invested over C$129 billion since 2016 through the Investing in Canada Plan with an additional C$51 billion to be invested over the next five years (Infrastructure Canada, 2022). This shows that the federal government is willing to invest in large-scale infrastructure projects and intends to continue to do so in the future.

# Chapter 8

# Areas for Further Research

The majority of reservoir data in our study area is comprised of data points located some distance away from the location of the injection array. This is likely due to the data source being information obtained during the course of hydrocarbon exploration, such as through well logs and drillstem tests. While this provides ample data for regions that have been explored for hydrocarbon production, there is a lack of data in regions that are located away from oil and gas reservoirs. This represents a barrier when it comes to evaluating these regions to determine their potential for $CO_2$ sequestration, particularly when modeling the pressure evolution and $CO_2$ migration. Large-scale CCS systems would therefore benefit from data gathered in the vicinity of the potential injection array, particularly permeability and porosity data which can vary unpredictably across an aquifer. This data may enable the use of a three-dimensional computational model instead of the one-dimensional model used here.

We have evaluated the potential of $CO_2$ capture from the CCS hub, but the remaining oil sands emitters that are not part of the hub (Fig. 3.1) may also be

candidates for inclusion in a large-scale CCS system. These emitters were not included in this work because they are located some distance away from the CCS hub, but they still represent a significant source of emissions. While the mitigation potential of the CCS system proposed here is significant it is not sufficient to reach net-zero and more action, such as the inclusion of additional large emitters in a provincial-scale CCS system, is required to reach this target.

## 8.1 Effects of Uncertain Parameters

There are two factors that introduce an element of uncertainty to our results: 1) Some of the parameters used in our modeling are average/representative values for the study area, and 2) The sheer length of time required for the injected $CO_2$ to stop migrating and become completely trapped. Here, we qualitatively discuss the effects that changes to major parameters used in the modeling would have on our results, namely the storage capacity and system cost. We also discuss some possible events that could occur over the $CO_2$ migration period and their effects on our results, but at a very high level out of necessity since it is impossible to make accurate predictions over thousands of years.

The most important aquifer parameters are permeability, porosity, and initial pressure. Variations in permeability and porosity have direct impacts on the storage capacity. A higher permeability and/or porosity would result in a slower rate of increase of aquifer pressure as the $CO_2$ is injected, thus leading to an increased pressure-limited storage capacity. This would indirectly increase the cost of the system as the pipelines would need to be designed to a higher capacity. A lower permeability and/or porosity would have the opposite effect.

A higher initial aquifer pressure would result in a higher storage capacity as the injected $CO_2$ would occupy less space. However, this may also necessitate a lower injection rate due to a smaller permissible pressure increase over the injection period before the fracture pressure is reached. Thus, it is likely that higher aquifer pressure would result in a decrease in the injection rate but an increase in the amount of $CO_2$ that can ultimately be stored in the same volume of space. This would likely reduce the cost of the system as the maximum capacity of the pipeline can be lower. A lower initial aquifer pressure would likely result in an increase in the permissible injection rate and cost.

Other relevant aquifer parameters include thickness, temperature, salinity, and depth. Higher thickness permits an increased injection rate (and thus higher storage capacity). A lower thickness would result in a decreased injection rate and storage capacity. Higher temperatures and salinities would decrease the storage capacity, while lower temperatures and salinities would increase the storage capacity. The initial pressure varies with injection well depth, with the effects noted above. These effects would all indirectly affect cost through the required pipeline capacity.

There are also variables that affect the configuration of the pipeline network and thus cost, either through pipeline length or capacity. The approval of new pipeline rights-of-way could enable the use of a more direct route and thus lower the cost. Conversely, if for any reason the use of certain rights-of-way is not approved, a less direct route would need to be used and the cost would increase. Since the aquifers slope upwards from the injection array to the emission sources, changes to the regulatory minimum $CO_2$ storage depth would either enable injection to occur closer to the emission sources and thus decrease cost, or force the injection array to be located

further away with a corresponding increase in cost.

Lastly, the maximum duration for $CO_2$ to become permanently trapped in our system is 11000 years. Any number of events, both natural and anthropogenic, could occur over this time frame that have an effect on our system. The effects of anthropogenic events would be primarily relevant during the injection period as it is more difficult for events of this nature to have an effect on subsurface $CO_2$. The anthropogenic event with the largest potential impact is likely to be governmental policy changes, whether favourable or unfavourable. Favourable policy changes could include an increased emphasis on the need for emission reduction through $CO_2$ sequestration as Canada approaches its 2030 emission reduction targets, which could lead to stronger policy incentives that would enable CCS on an even larger scale. Unfavourable policy changes could include disincentives against the construction of a new pipeline due to public opinion.

Natural events are relevant throughout the entire injection and migration period and take the form of natural disasters, which are becoming increasingly common due to the effects of climate change. The primary natural disaster that would affect the subsurface is an earthquake. Although the majority of seismic activity occurs at the coast and Alberta is located inland, there is still a nonzero possibility of an earthquake in Alberta before the $CO_2$ is completely trapped. If this occurs during the injection period, it would likely lead to a pause in $CO_2$ capture and injection while repairs are carried out. If this occurs during the migration period, an earthquake of sufficient magnitude could cause adverse effects on the aquifers.

# Chapter 9

# Conclusion

The Royal Bank of Canada estimates that C$2 trillion must be invested over the next 30 years (Environment and Climate Change Canada, 2022a; RBC, 2021) to achieve net-zero emissions. This sum is equivalent to C$60 billion per year, which is also subject to increase with inflation. The most recent modeling suggests that a 491 Mt gap remains between projected Canadian emissions in 2030 and net-zero emissions in 2050 (Environment and Climate Change Canada, 2022b). The CCS system we propose will sequester 1913 Mt of $CO_2$ over the period between 2030-2100, based on the projected capturable $CO_2$ emissions (Fig. 3.3) over that period from a hub of large emitters in the Athabasca oil sands. This volume is less than the pressure-limited capacity of the Nisku and Wabamun saline aquifers (Fig. 4.2) and can thus be stored safely. The CCS system is projected to sequester 48.09 Mt of $CO_2$ in 2050, equivalent to 10% of the projected emissions gap. The storage of this amount of $CO_2$ will be possible at a total capital cost of 0.19% of the estimated investment required to achieve net-zero. This shows that the proposed CCS system has the potential to reduce $CO_2$ emissions at a level which far outweighs its cost.

Our work provides a comprehensive framework which can be used to design and evaluate future large-scale CCS systems. This framework is necessary because it provides a holistic approach that considers all the elements of a CCS system that are necessary for success, namely the capture, transport, and storage aspects, the associated costs and financing, and the necessary regulatory and policy requirement. Careful and due consideration of every element of a CCS system is necessary to ensure the long-term success of the system.

# Appendix A

# Pipeline Engineering Inputs

This Appendix contains the engineering inputs used for the NETL $CO_2$ Transport Cost Model.

Table A.1: Engineering inputs used in the NETL $CO_2$ Transport Cost Model.

| Parameter | Value | Source |
|---|---|---|
| Annual $CO_2$ transported | Varies for each segment | |
| Capacity factor | 100% | |
| Pipeline length | varies | ArcGIS Pro |
| Pipeline diameter | varies | Equation 6.0.1 |
| Inlet pressure | 2100 psi | Edwards & Celia (2018) |
| Outlet pressure | 1400 psi | Edwards & Celia (2018) |
| Elevation change | Varies | ArcGIS Pro |
| Ground temperature | 5 C | Toogood (1976) |
| Pump efficiency | 75% | McCollum & Ogden (2006) |

# Bibliography

AER (1994). Directive 051: Injection and disposal wells.

Alberta Department of Energy (2020). *Quest Carbon Capture and Storage Project Annual Summary Report*. Report. URL: https://open.alberta.ca/dataset/f74375f3-3c73-4b9c-af2b-ef44e59b7890/resource/ff260985-e616-4d2e-92e0-9b91f5590136/download/energy-quest-annual-summary-alberta-department-of-energy-2019.pdf.

Alberta Geological Survey (1994a). *Atlas of the Western Canada Sedimentary Basin: Chapter 12 - Devonian Woodbend-Winterburn Strata*. Technical Report Alberta Energy Regulator.

Alberta Geological Survey (1994b). Atlas of the western canada sedimentary basin: Chapter 13 - devonian wabamun group.

Alberta Geological Survey, & Alberta Energy Regulator (2021). Geological framework of alberta.

Alcalde, J., Heinemann, N., Mabon, L., Worden, R. H., de Coninck, H., Robertson, H., Maver, M., Ghanbari, S., Swennenhuis, F., Mann, I., Walker, T., Gomersal,

S., Bond, C. E., Allen, M. J., Haszeldine, R. S., James, A., Mackay, E. J., Brownsort, P. A., Faulkner, D. R., & Murphy, S. (2019). Acorn: Developing full-chain industrial carbon capture and storage in a resource- and infrastructure-rich hydrocarbon province. *Journal of Cleaner Production*, *233*, 963–971. URL: https://www.sciencedirect.com/science/article/pii/S0959652619320426. doi:10.1016/j.jclepro.2019.06.087.

Anderson, S., & Newell, R. (2004). Prospects for carbon capture and storage technologies. *Annual Review of Environment and Resources*, *29*, 109–142. URL: https://dx.doi.org/10.1146/annurev.energy.29.082703.145619. doi:10.1146/annurev.energy.29.082703.145619.

Bachu, S. (2007). Carbon dioxide storage capacity in uneconomic coal beds in Alberta, Canada: Methodology, potential and site identification. *International Journal of Greenhouse Gas Control*, *1*, 374–385. URL: https://www.sciencedirect.com/science/article/pii/S1750583607000709. doi:10.1016/S1750-5836(07)00070-9.

Bachu, S. (2015). Review of $CO_2$ storage efficiency in deep saline aquifers. *International Journal of Greenhouse Gas Control*, *40*, 188–202. URL: https://www.sciencedirect.com/science/article/pii/S1750583615000146. doi:10.1016/j.ijggc.2015.01.007.

Bachu, S. (2016). Identification of oil reservoirs suitable for co2-eor and co2 storage (ccus) using reserves databases, with application to alberta, canada. *International Journal of Greenhouse Gas Control*, .

Bachu, S., Bistran, R., & Jafari, A. (2014a). *Identification of Options for CO2 Storage in the Athabasca Area, Alberta*. Report Alberta Innovates.

Bachu, S., Melnik, A., & Bistran, R. (2014b). Approach to evaluating the $CO_2$ storage capacity in devonian deep saline aquifers for emissions from oil sands operations in the athabasca area, canada. *Energy Procedia*, *63*, 5093–5102. URL: https://dx.doi.org/10.1016/j.egypro.2014.11.539. doi:10.1016/j.egypro.2014.11.539.

Bäckstrand, K., Meadowcroft, J., & Oppenheimer, M. (2011). The politics and policy of carbon capture and storage: Framing an emergent technology. *Global Environmental Change*, *21*, 275–281. URL: https://www.sciencedirect.com/science/article/pii/S0959378011000355. doi:10.1016/j.gloenvcha.2011.03.008.

Balaji, K., & Rabiei, M. (2022). Carbon dioxide pipeline route optimization for carbon capture, utilization, and storage: A case study for north-central USA. *Sustainable Energy Technologies and Assessments*, *51*, 101900. doi:10.1016/J.SETA.2021.101900.

Bandilla, K. W., Guo, B., & Celia, M. A. (2019). A guideline for appropriate application of vertcially-integrated modeling approaches for geologic carbon storage modeling. *International Journal of Greenhouse Gas Control*, *91*, 102808.

Bank of Canada (2016). Renewal of the inflation-control target. URL: https://www.bankofcanada.ca/wp-content/uploads/2016/10/background_nov11.pdf.

Bank of Canada (2022). Annual exchange rates.

Bell, J., & Bachu, S. (2003). In situ stress magnitude and orientation estimates for Cretaceous coal-bearing strata beneath the plains area of central and southern Alberta. *Bulletin of Canadian Petroleum Geology*, *51*, 1–28. URL: https://doi.org/10.2113/gscpgbull.51.1.1. doi:10.2113/gscpgbull.51.1.1. arXiv:https://pubs.geoscienceworld.org/cspg/bcpg/article-pdf/51/1/1/3312160/1.pd

Bennion, D. B., & Bachu, S. (2008). Drainage and imbibition relative permeability relationships for supercritical co2/brine and h2s/brine systems in intergranular sandstone, carbonate, shale, and anhydrite rocks. *SPE Reservoir Evaluation & Engineering*, *11*, 487–496.

Boot-Handford, M. E., Abanades, J. C., Anthony, E. J., Blunt, M. J., Brandani, S., Mac Dowell, N., Fernández, J. R., Ferrari, M.-C., Gross, R., Hallett, J. P., Haszeldine, R. S., Heptonstall, P., Lyngfelt, A., Makuch, Z., Mangano, E., Porter, R. T. J., Pourkashanian, M., Rochelle, G. T., Shah, N., Yao, J. G., & Fennell, P. S. (2014). Carbon capture and storage update. *Energy and Environmental Science*, *7*, 130–189. URL: http://dx.doi.org/10.1039/C3EE42350F. doi:10.1039/C3EE42350F.

Budinis, S., Krevor, S., Dowell, N. M., Brandon, N., & Hawkes, A. (2018). An assessment of CCS costs, barriers and potential. *Energy Strategy Reviews*, *22*, 61–81. URL: https://www.sciencedirect.com/science/article/pii/S2211467X18300634. doi:10.1016/j.esr.2018.08.003.

Bui, M., Adjiman, C. S., Bardow, A., Anthony, E. J., Boston, A., Brown, S., Fennell, P. S., Fuss, S., Galindo, A., Hackett, L. A., Hallett, J. P., Herzog, H. J., Jackson, G., Kemper, J., Krevor, S., Maitland, G. C., Matuszewski, M., Metcalfe, I. S., Petit, C., Puxty, G., Reimer, J., Reiner, D. M., Rubin, E. S., Scott, S. A., Shah, N., Smit, B.,

Trusler, J. P. M., Webley, P., Wilcox, J., & Mac Dowell, N. (2018). Carbon capture and storage (CCS): the way forward. *Energy and Environmental Science*, *11*, 1062–1176. URL: http://dx.doi.org/10.1039/C7EE02342A. doi:10.1039/C7EE02342A.

Bureau of Labor Statistics (2022). Cpi inflation calculator.

CAPP (2021). Oil sands production. URL: https://www.capp.ca/resources/statistics/.

Chao, C., Deng, Y., Dewil, R., Baeyens, J., & Fan, X. (2021). Post-combustion carbon capture. *Renewable and Sustainable Energy Reviews*, *138*, 110490–110490. URL: https://www.sciencedirect.com/science/article/pii/S1364032120307760. doi:10.1016/j.rser.2020.110490.

Ciotta, M., Peyerl, D., Zacharias, L. G. L., Fontenelle, A. L., Tassinari, C., & Moretto, E. M. (2021). $CO_2$ storage potential of offshore oil and gas fields in Brazil. *International Journal of Greenhouse Gas Control*, *112*, 103492–103492. URL: https://www.sciencedirect.com/science/article/pii/S1750583621002449. doi:10.1016/j.ijggc.2021.103492.

Clark, A. J., Lake, L. W., & Patzek, T. W. (2011). Production forecasting with logistic growth models. *Proceedings - SPE Annual Technical Conference and Exhibition*, *1*, 184–194. doi:10.2118/144790-MS.

Cole, S., & Itani, S. (2013). The Alberta Carbon Trunk Line and the benefits of $CO_2$. *Energy Procedia*, *37*, 6133–6139. URL: https://www.sciencedirect.com/science/article/pii/S1876610213007856. doi:10.1016/j.egypro.2013.06.542.

Congressional Research Service (2021). The tax credit for carbon sequestration (Section 45Q). URL: https://crsreports.congress.gov.

Department of Finance Canada (). Legislative proposals relating to income tax and other legislation.

Department of the Environment (2020). Clean fuel regulations. URL: https://gazette.gc.ca/rp-pr/p1/2020/2020-12-19/html/reg2-eng.html.

Duong, C., Bower, C., Hume, K., Rock, L., & Tessarolo, S. (2019). Quest carbon capture and storage offset project: Findings and learnings from 1st reporting period. *International Journal of Greenhouse Gas Control*, *89*, 65–75. URL: https://www.sciencedirect.com/science/article/pii/S1750583618307904. doi:10.1016/j.ijggc.2019.06.001.

Edwards, R. W. J., & Celia, M. A. (2018). Infrastructure to enable deployment of carbon capture, utilization, and storage in the United States. *Proceedings of the National Academy of Sciences*, *115*, E8815–E8824. URL: https://www.pnas.org/content/pnas/115/38/E8815.full.pdf. doi:10.1073/pnas.1806504115.

Eisinger, C. L., Lavoie, R., & Keith, D. W. (2011). The Wabamun Area Sequestration Project (WASP): A multidisciplinary study of gigaton scale $CO_2$ storage in a deep saline carbonate aquifer. *Energy Procedia*, *4*, 4793–4797. URL: https://www.sciencedirect.com/science/article/pii/S1876610211007235. doi:10.1016/j.egypro.2011.02.444.

Enhance Energy Inc, Wolf Carbon Solutions, & North West Redwater Partnership (2020). *Knowledge Sharing Report*. Report. URL: https:

//open.alberta.ca/dataset/90f61413-0ef1-45a4-9e1c-6bff7c23fd7e/resource/c67b52dd-90b2-4159-b14c-5729ecb9eeaf/download/energy-actl-knowledge-sharing-2019-detailed-report.pdf.

Environment and Climate Change Canada (2020). A healthy environment and a healthy economy. URL: https://www.canada.ca/content/dam/eccc/documents/pdf/climate-change/climate-plan/healthy_environment_healthy_economy_plan.pdf.

Environment and Climate Change Canada (2021a). Annex: Modelling and analysis of A Healthy Environment and a Healthy Economy. URL: https://www.canada.ca/en/services/environment/weather/climatechange/climate-plan/climate-plan-overview/healthy-environment-healthy-economy/annex-modelling-analysis.html.

Environment and Climate Change Canada (2021b). Canada's Climate Actions for a Healthy Environment and a Healthy Economy. URL: https://www.canada.ca/en/services/environment/weather/climatechange/climate-plan/climate-plan-overview/actions-healthy-environment-economy.html.

Environment and Climate Change Canada (2021c). Greenhouse gas sources and sinks: executive summary 2021. URL: https://www.canada.ca/en/environment-climate-change/services/climate-change/greenhouse-gas-emissions/sources-sinks-executive-summary-2021.html#toc2.

Environment and Climate Change Canada (2021d). Progress towards Canada's greenhouse gas emissions reduction target. URL: https://www.canada.ca/

en/environment-climate-change/services/environmental-indicators/progress-towards-canada-greenhouse-gas-emissions-reduction-target.html.

Environment and Climate Change Canada (2022a). 2030 emissions reduction plan.

Environment and Climate Change Canada (2022b). Canada's eighth national communication on climate change and fifth biennial report.

Ettehadtavakkol, A., Lake, L. W., & Bryant, S. L. (2014). Co2-eor and storage design optimization. *International Journal of Greenhouse Gas Control*, *25*, 79–92. URL: https://www.sciencedirect.com/science/article/pii/S1750583614000899. doi:https://doi.org/10.1016/j.ijggc.2014.04.006.

Falkowski, P., Scholes, R. J., Boyle, E., Canadell, J., Canfield, D., Elser, J., Gruber, N., Hibbard, K., Högberg, P., Linder, S., Mackenzie, F. T., Moore, B. I. I. I., Pedersen, T., Rosenthal, Y., Seitzinger, S., Smetacek, V., & Steffen, W. (2000). The Global Carbon Cycle: A Test of Our Knowledge of Earth as a System. *Science*, *290*, 291–296. URL: https://www.science.org/doi/abs/10.1126/science.290.5490.291. doi:10.1126/science.290.5490.291.

Ghaderi, S., & Leonenko, Y. (2015). Reservoir modeling for wabamun lake sequestration project. *Energy Science and Engineering*, .

Goodarzi, S., Settari, A., & Keith, D. (2012). Geomechanical modeling for co2 storage in nisku aquifer in wabamun lake area in canada. *International Journal of Greenhouse Gas Control*, .

Goodman, A., Hakala, A., Bromhal, G., Deel, D., Rodosta, T., Frailey, S., Small, M., Allen, D., Romanov, V., Fazio, J., Huerta, N., McIntyre, D., Kutchko, B., & Guthrie, G. (2011). U.S. DOE methodology for the development of geologic storage potential for carbon dioxide at the national and regional scale. *International Journal of Greenhouse Gas Control*, *5*, 952–965. URL: https://www.sciencedirect.com/science/article/pii/S1750583611000405. doi:10.1016/j.ijggc.2011.03.010.

Government of Alberta (2020). Technology Innovation and Emissions Reduction Regulation. URL: https://www.qp.alberta.ca/1266.cfm?page=2019_133.cfm&leg_type=Regs&isbncln=9780779818501.

Government of Alberta (2021). Request for Full Project Proposals for Carbon Sequestration Hubs. URL: https://www.alberta.ca/assets/documents/energy-request-for-full-project-proposals-rfpp-guidelines.pdf.

Government of Canada (2021a). Budget 2021. URL: https://www.budget.gc.ca/2021/home-accueil-en.html.

Government of Canada (2021b). Greenhouse Gas Reporting Program (GHGRP) - Facility Greenhouse Gas (GHG) Data. URL: https://open.canada.ca/data/en/dataset/a8ba14b7-7f23-462a-bdbb-83b0ef629823.

Government of Canada (2021c). Net Zero Accelerator Initiative - Strategic Innovation Fund. URL: https://www.ic.gc.ca/eic/site/125.nsf/eng/00039.html.

Government of Canada (2022). What is the clean fuel standard? URL: https://www.canada.ca/en/environment-climate-change/services/managing-pollution/

energy-production/fuel-regulations/clean-fuel-standard/about.html#toc0.

Hansen, J., & Sato, M. (2004). Greenhouse gas growth rates. *Proceedings of the National Academy of Sciences of the United States of America*, *101*, 16109–16114. URL: https://www.pnas.org/content/pnas/101/46/16109.full.pdf. doi:10.1073/pnas.0406982101.

Hasan, M. M. F., First, E. L., Boukouvala, F., & Floudas, C. A. (2015). A multi-scale framework for $CO_2$ capture, utilization, and sequestration: CCUS and CCU. *Computers and Chemical Engineering*, *81*, 2–21. URL: https://www.sciencedirect.com/science/article/pii/S0098135415001350. doi:10.1016/j.compchemeng.2015.04.034.

Haszeldine, R. S. (2009). Carbon capture and storage: How green can black be? *Science*, *325*, 1647–1652. URL: https://www.science.org/doi/abs/10.1126/science.1172246. doi:10.1126/science.1172246.

Heddle, G., Herzog, H., & Klett, M. (2003). *The Economics of $CO_2$ Storage*. Report. URL: http://lfee.mit.edu/publications/.

Heidaryan, E., Hatami, T., Rahimi, M., & Moghadasi, J. (2011). Viscosity of pure carbon dioxide at supercritical region: Measurement and correlation approach. *The Journal of Supercritical Fluids*, *56*, 144–151. doi:10.1016/J.SUPFLU.2010.12.006.

Hesse, M. A., Orr, F. M., Jr., & Tchelepi, H. A. (2008). Gravity currents with residual trapping, . *611*, 35–60.

Hidalgo, J. J., MacMinn, C. W., & Juanes, R. (2013). Dynamics of convective dissolution from a migrating current of carbon dioxide. *Advances in Water Resources*, *62*, 511–519.

Hubbert, M. K. (1956). *Nuclear Energy and the Fossil Fuels*. Report. URL: `http://www.energycrisis.com/Hubbert/1956/1956.pdf`.

Infrastructure Canada (2016). Infrastructure Canada projects since 2002 - National.

Infrastructure Canada (2022). Investing in Canada Plan – Building a Better Canada. URL: `https://www.infrastructure.gc.ca/plan/about-invest-apropos-eng.html`.

International Energy Agency (2020). *CCUS in Clean Energy Transitions*. Report. URL: `https://www.iea.org/reports/ccus-in-clean-energy-transitions`.

IPCC (2014). *CARBON DIOXIDE CAPTURE AND STORAGE*. Report. URL: `https://www.ipcc.ch/site/assets/uploads/2018/03/srccs_wholereport-1.pdf`.

IPCC (2018). Summary for policymakers. in: Global warming of 1.5c. an ipcc special report on the impacts of global warming of 1.5c above pre-industrial levels and related global greenhouse gas emission pathways, in the context of strengthening the global response to the threat of climate change, sustainable development, and efforts to eradicate poverty.

Jensen, M. D., Pei, P., Snyder, A. C., Heebink, L. V., Gorecki, C. D., Steadman, E. N., & Harju, J. A. (2013). A Phased Approach to Building a Hypothetical Pipeline Network for $CO_2$ Transport During CCUS. *Energy Procedia*,

*37*, 3097–3104. URL: https://www.sciencedirect.com/science/article/pii/S1876610213004384. doi:10.1016/j.egypro.2013.06.195.

Juanes, R., MacMinn, C. W., & Szulczewski, M. L. (2010). The footprint of the CO2 plume during carbon dioxide storage in saline aquifers: storage efficiency for capillary trapping at the basin scale,. *Transport in porous media*, *82*, 19–30.

Kazemifar, F. (2021). A review of technologies for carbon capture, sequestration, and utilization: Cost, capacity, and technology readiness. *Greenhouse Gases: Science and Technology*, . URL: https://onlinelibrary.wiley.com/doi/full/10.1002/ghg.2131https://onlinelibrary.wiley.com/doi/abs/10.1002/ghg.2131https://onlinelibrary.wiley.com/doi/10.1002/ghg.2131. doi:10.1002/GHG.2131.

Kearns, D., Liu, H., & Consoli, C. (2021). *Technology Readiness and Costs of CCS*. Report. URL: https://www.globalccsinstitute.com/wp-content/uploads/2021/03/Technology-Readiness-and-Costs-for-CCS-2021-1.pdf.

Kennedy, C., Steinberger, J., Gasson, B., Hansen, Y., Hillman, T., Havránek, M., Pataki, D., Phdungsilp, A., Ramaswami, A., & Mendez, G. V. (2009). Greenhouse gas emissions from global cities. *Environmental Science and Technology*, *43*, 7297–7302. URL: https://doi.org/10.1021/es900213p. doi:10.1021/es900213p.

Klyukin, Y. I., Lowell, R. P., & Bodnar, R. J. (2017). A revised empirical model to calculate the dynamic viscosity of $H_2O$ NaCl fluids at elevated temperatures and pressures ($\leq$ 1000°C, $\leq$ 500MPa, 0–100 wt % NaCl). *Fluid Phase Equilibria*, *433*, 193–205. URL: https://dx.doi.org/10.1016/j.fluid.2016.11.002. doi:10.1016/j.fluid.2016.11.002.

Kuby, M. J., Middleton, R. S., & Bielicki, J. M. (2011). Analysis of cost savings from networking pipelines in CCS infrastructure systems. *Energy Procedia*, *4*, 2808–2815. doi:10.1016/J.EGYPRO.2011.02.185.

Leonzio, G., Foscolo, P. U., & Zondervan, E. (2019). An outlook towards 2030: Optimization and design of a CCUS supply chain in Germany. *Computers and Chemical Engineering*, *125*, 499–513. URL: https://www.sciencedirect.com/science/article/pii/S0098135418310883. doi:10.1016/j.compchemeng.2019.04.001.

Leung, D. Y. C., Caramanna, G., & Maroto-Valer, M. M. (2014). An overview of current status of carbon dioxide capture and storage technologies. *Renewable and Sustainable Energy Reviews*, *39*, 426–443. URL: https://www.sciencedirect.com/science/article/pii/S1364032114005450. doi:10.1016/j.rser.2014.07.093.

Liang, Z., Rongwong, W., Liu, H., Fu, K., Gao, H., Cao, F., Zhang, R., Sema, T., Henni, A., Sumon, K., Nath, D., Gelowitz, D., Srisang, W., Saiwan, C., Benamor, A., Al-Marri, M., Shi, H., Supap, T., Chan, C., Zhou, Q., Abu-Zahra, M., Wilson, M., Olson, W., Idem, R., & Tontiwachwuthikul, P. (2015). Recent progress and new developments in post-combustion carbon-capture technology with amine based solvents. *International Journal of Greenhouse Gas Control*, *40*, 26–54. doi:10.1016/J.IJGGC.2015.06.017. (Henry) (PT).

MacDowell, N., Florin, N., Buchard, A., Hallett, J., Galindo, A., Jackson, G., Adjiman, C. S., Williams, C. K., Shah, N., & Fennell, P. (2010). An overview of $CO_2$ capture technologies. *Energy and Environmental Science*,

*3*, 1645–1669. URL: https://pubs.rsc.org/en/content/articlehtml/2010/ee/c004106h. doi:10.1039/C004106H.

MacMinn, C. W., Szulczewski, M. L., & Juanes, R. (2011). $CO_2$ migration in saline aquifers. Part 2: Capillary and solubility trapping. *Journal of Fluid Mechanics*, *688*.

McCollum, D., & Ogden, J. (2006). *Techno-Economic Models for Carbon Dioxide Compression, Transport, and Storage and Correlations for Estimating Carbon Dioxide Density and Viscosity*. Report. URL: https://itspubs.ucdavis.edu/publication_detail.php?id=1047.

Metz, B., Davidson, O., De Coninck, H., Loos, M., & Meyer, L. (2005). *IPCC special report on carbon dioxide capture and storage*. Cambridge: Cambridge University Press.

Mokhtar, M., Ali, M. T., Khalilpour, R., Abbas, A., Shah, N., Hajaj, A. A., Armstrong, P., Chiesa, M., & Sgouridis, S. (2012). Solar-assisted post-combustion carbon capture feasibility study. *Applied Energy*, *92*, 668–676. doi:10.1016/J.APENERGY.2011.07.032.

National Oceanic and Atmospheric Administration (2023). Trends in atmospheric carbon dioxide. URL: https://gml.noaa.gov/ccgg/trends/.

Nordbotten, J. M., Celia, M. A., & Bachu, S. (2005). Injection and storage of $CO_2$ in deep saline aquifers: Analytical solution for $CO_2$ plume evolution during injection. *Transport in Porous media*, *58*, 339–360.

NPC (2019). Meeting the dual challenge: A roadmap to at-scale deployment of carbon capture, use, and storage. URL: https://dualchallenge.npc.org.

Nygaard, R., & Lavoie, R. (2009). *Energy and Environmental Systems Group Institute for Sustainable Energy, Environment and Economy (ISEEE) Project Cost Estimate Wabamun Area CO 2 Sequestration Project (WASP)*. Report.

Ordorica-Garcia, G., Wong, S., & Faltinson, J. (2011). Characterisation of $CO_2$ emissions in canada's oil sands industry: Estimating the future $CO_2$ supply and capture cost curves. *Energy Procedia*, *4*, 2637–2644. URL: https://dx.doi.org/10.1016/j.egypro.2011.02.163. doi:10.1016/j.egypro.2011.02.163.

Osman, A. I., Hefny, M., Abdel Maksoud, M. I. A., Elgarahy, A. M., & Rooney, D. W. (2021). Recent advances in carbon capture storage and utilisation technologies: a review. *Environmental Chemistry Letters*, *19*, 797–849. URL: https://doi.org/10.1007/s10311-020-01133-3. doi:10.1007/s10311-020-01133-3.

Ouyang, L.-B. (2011). New correlations for predicting the density and viscosity of supercritical carbon dioxide under conditions expected in carbon capture and sequestration operations. *The Open Petroleum Engineering Journal*, *4*, 13–21.

Parker, N. (2004). *Using Natural Gas Transmission Pipeline Costs to Estimate Hydrogen Pipeline Costs*. Report. URL: https://itspubs.ucdavis.edu/publication_detail.php?id=197.

Parliamentary Budget Officer (2022). Federal infrastructure spending, 2016-17 to 2026-27.

Pau, G. S., Bell, J. B., Pruess, K., Almgren, A. S., Lijewski, M. J., & Zhang, K. (2010). High-resolution simulation and characterization of density-driven flow in CO2 storage in saline aquifers. *Advances in Water Resources*, *33*, 443–455.

Peletiri, S. P., Rahmanian, N., & Mujtaba, I. M. (2018). $CO_2$ pipeline design: A review. *Energies 2018, Vol. 11, Page 2184*, *11*, 2184–2184. URL: https://www.mdpi.com/1996-1073/11/9/2184/htmhttps://www.mdpi.com/1996-1073/11/9/2184. doi:10.3390/EN11092184.

Pilorgé, H., McQueen, N., Maynard, D., Psarras, P., He, J., Rufael, T., & Wilcox, J. (2020). Cost Analysis of Carbon Capture and Sequestration of Process Emissions from the U.S. Industrial Sector. *Environmental Science and Technology*, *54*, 7524–7532. URL: https://dx.doi.org/10.1021/acs.est.9b07930. doi:10.1021/acs.est.9b07930.

Pinder, G. F., & Gray, W. G. (2008). *Essentials of multiphase flow and transport in porous media*. John Wiley & Sons.

Porter, R. T. J., Fairweather, M., Kolster, C., Mac Dowell, N., Shah, N., & Woolley, R. M. (2017). Cost and performance of some carbon capture technology options for producing different quality $CO_2$ product streams. *International Journal of Greenhouse Gas Control*, *57*, 185–195. doi:10.1016/j.ijggc.2016.11.020.

Potkins, M. (2022). Alberta's industrial carbon tax to triple by 2030 to match ottawa's minimum standards.

Raza, A., Gholami, R., Rezaee, R., Rasouli, V., & Rabiei, M. (2019). Significant aspects of carbon capture and storage – a review. *Petroleum*,

*5*, 335–340. URL: https://www.sciencedirect.com/science/article/pii/S2405656118301366. doi:10.1016/j.petlm.2018.12.007.

RBC (2021). The $2 trillion transition: Canada's road to net zero.

Ringrose, P. S., Furre, A.-K., Gilfillan, S. M., Krevor, S., Landrø, M., Leslie, R., Meckel, T., Nazarian, B., & Zahid, A. (2021). Storage of carbon dioxide in saline aquifers: Physicochemical processes, key constraints, and scale-up potential. *Annual Review of Chemical and Biomolecular Engineering*, *12*, 471–494. URL: https://doi.org/10.1146/annurev-chembioeng-093020-091447. doi:10.1146/annurev-chembioeng-093020-091447. arXiv:https://doi.org/10.1146/annurev-chembioeng-093020-091447. PMID: 33872518.

Rockström, J., Steffen, W., Noone, K., Persson, Å., Chapin, F. S., Lambin, E. F., Lenton, T. M., Scheffer, M., Folke, C., Schellnhuber, H. J., Nykvist, B., de Wit, C. A., Hughes, T., van der Leeuw, S., Rodhe, H., Sörlin, S., Snyder, P. K., Costanza, R., Svedin, U., Falkenmark, M., Karlberg, L., Corell, R. W., Fabry, V. J., Hansen, J., Walker, B., Liverman, D., Richardson, K., Crutzen, P., & Foley, J. A. (2009). A safe operating space for humanity. *Nature*, *461*, 472–475. URL: https://doi.org/10.1038/461472a. doi:10.1038/461472a.

Romasheva, N., & Ilinova, A. (2019). CCS Projects: How Regulatory Framework Influences Their Deployment. *Resources*, *8*, 181–181. URL: https://www.mdpi.com/2079-9276/8/4/181. doi:10.3390/resources8040181.

Smith, E., Morris, J., Kheshgi, H., Teletzke, G., Herzog, H., & Paltsev, S. (2021). The cost of $CO_2$ transport and storage in global integrated assessment modeling.

*International Journal of Greenhouse Gas Control*, *109*, 103367. doi:10.1016/J.IJGGC.2021.103367.

Sorrell, S., & Speirs, J. (2019). *UKERC Review of Evidence for Global Oil Depletion. Technical Report 5: Methods of estimating ultimately recoverable resources*. Report. URL: https://ukerc8.dl.ac.uk/UCAT/PUBLICATIONS/UKERC_Review_of_Evidence_on_Global_Oil_Depletion-Technical_Report_5-Methods_of_estimating_ultimately_recoverable_resources.pdf.

Szulczewski, M. L., Macminn, C. W., Herzog, H. J., & Juanes, R. (2012). Lifetime of carbon capture and storage as a climate-change mitigation technology. *Proceedings of the National Academy of Sciences*, *109*, 5185–5189. URL: https://dx.doi.org/10.1073/pnas.1115347109. doi:10.1073/pnas.1115347109.

Szulczewski, M. L., MacMinn, C. W., & Juanes, R. (2014). Theoretical analysis of how pressure buildup and CO2 migration can both constrain storage capacity in deep saline aquifers. *International Journal of Greenhouse Gas Control*, *23*, 113–118.

Tapia, J. F. D., Lee, J.-Y., Ooi, R. E. H., Foo, D. C. Y., & Tan, R. R. (2018). A review of optimization and decision-making models for the planning of $CO_2$ capture, utilization and storage (CCUS) systems. *Sustainable Production and Consumption*, *13*, 1–15. URL: https://www.sciencedirect.com/science/article/pii/S2352550917300453. doi:10.1016/j.spc.2017.10.001.

Toogood, J. A. (1976). Deep Soil Temperatures at Edmonton. *Canadian Journal of Soil Science*, *56*, 505–506. doi:10.4141/cjss76-060.

United Nations (2015). Paris Agreement. URL: https://unfccc.int/sites/default/files/english_paris_agreement.pdf.

USDOE (2018). *FE/NETL CO2 Transport Cost Model*. Report U.S. Department of Energy. URL: https://www.osti.gov/biblio/1556911-fe-netl-co2-transport-cost-model-description-user-manual.

WorleyParsons (2003). *Baseline Hydrogeology Assessment*. Report. URL: https://open.alberta.ca/dataset/9625726c-66b5-4673-954a-8e96b67b6637/resource/f05520e4-01f6-43be-8708-7ddb3f03a395/download/BASELINE-HYDROGEOLOGY-ASSESSMENT.pdf.

Yao, X., Zhong, P., Zhang, X., & Zhu, L. (2018). Business model design for the carbon capture utilization and storage (CCUS) project in China. *Energy Policy*, *121*, 519–533. URL: https://www.sciencedirect.com/science/article/pii/S0301421518304075. doi:10.1016/j.enpol.2018.06.019.

Yu, S., Horing, J., Liu, Q., Dahowski, R., Davidson, C., Edmonds, J., Liu, B., Mcjeon, H., McLeod, J., Patel, P., & Clarke, L. (2019). CCUS in China's mitigation strategy: insights from integrated assessment modeling. *International Journal of Greenhouse Gas Control*, *84*, 204–218. doi:10.1016/J.IJGGC.2019.03.004.

Zanco, S. E., Pérez-Calvo, J.-F., Gasós, A., Cordiano, B., Becattini, V., & Mazzotti, M. (2021). Postcombustion $CO_2$ capture: A comparative techno-economic assessment of three technologies using a solvent, an adsorbent, and a membrane. *ACS Engineering Au*, *1*, 50–72. URL: https://doi.org/10.1021/acsengineeringau.1c00002. doi:10.1021/acsengineeringau.1c00002.